

Spin-wave turbulence beyond the parametric excitation threshold

V. E. Zakharov, V. S. L'vov, and S. S. Starobinets

L.D. Landau Institute of Theoretical Physics, USSR Academy of Sciences, Chernogolovka (Moscow District)
Usp. Fiz. Nauk 114, 609–654 (December 1974)

The nonlinear stage of the parametric excitation of spin waves in ferromagnetic dielectrics is reviewed. The main nonlinear mechanism which limits the amplitude of the exponentially growing waves is the "pairing" of waves with equal and opposite wave vectors, which leads to the violation of phase relationships. This effect is described in terms of a Hamiltonian which is diagonal in the wave pairs; The corresponding approximation is called the S theory. Within the framework of this theory, the distribution of the excited waves in k space is singular: the waves lie on individual lines or points. Consequences of the S theory and their experimental verification are discussed in detail. Collective oscillations of a spin-wave system and the origin of the observed self-modulation of their amplitude are also considered.

CONTENTS

1. Introduction	896
2. Parametric Instability in Ferromagnets	898
3. The Stationary Post-Threshold State. The S Theory and its Comparison with Experiment	902
4. Collective Excitations and Auto-Oscillations of Magnetization	909
5. Other Problems in Spin-Wave Turbulence	914
6. Conclusion	917

1. INTRODUCTION

There has been increased interest during the last decade in phenomena taking place in nonlinear media during the excitation and interaction in them of finite-amplitude waves (see, for example, the review^[1]). One can even speak of a new branch of physics, namely, the physics of waves in nonlinear media, in which wave processes in plasmas, ferromagnets, hydrodynamics, and a large part of nonlinear optics are treated from a unified point of view. A very common situation in nonlinear media is the simultaneous excitation and interaction of many noncoherent oscillatory degrees of freedom, where the energy distribution of these degrees of freedom is such that the system is not in any sense close to the state of thermodynamic equilibrium.

Such situations require statistical methods for their description, but are not fundamentally amenable to the traditional methods of statistical physics, and can be collectively described by the phrase "wave turbulence." When the phases of the individual waves can be looked upon as statistically independent (the minimum requirement for this is that the degree of nonlinearity is small), one speaks of weak turbulence. All other cases are classified as strong turbulence. From this point of view, "classical" turbulence must be looked upon as the limit of strong turbulence. The concept of "wave turbulence" (both weak and strong) defined in this way combines a multitude of different physical phenomena, the systematic study of which has only just begun.

Wave turbulence usually appears as a result of the development of some kind of instability. The present paper reviews theoretical and experimental results on a particular type of weak wave turbulence which is the result of the development in the medium of paramet-

ric instability (parametric resonance). A characteristic feature of this type of turbulence is that, in the simplest case, it is a purely dynamic problem, and considerable progress can be made toward its solution. The present review is largely concerned with the work of its authors. Other work is represented only to the extent to which it is relevant to the basic physical ideas developed in this review.

Parametric instability appears during the periodic variation (in time) of the parameters of the medium, or during the propagation through the medium of large-amplitude monochromatic waves. Since all the experimental results which we shall describe are concerned with the parametric excitation of spin waves in ferromagnets, we have included the phrase "spin waves" in the title of the paper although this type of turbulence can be realized in antiferromagnets, in plasmas, on the surface of liquids, and in other media.

The phenomenon of parametric resonance in an oscillator with one degree of freedom was discovered at the end of the 19th century (the Melde experiment) and was explained by Rayleigh^[2]. In the 1920s, parametric resonance was intensively investigated in connection with the newly developed subject of radio engineering. This period saw the development of the first parametric oscillators and amplifiers, and also the virtual completion (mainly by L. I. Mandel'shtam and his collaborators) of the development of the nonlinear theory of parametric resonance in systems with a small number of degrees of freedom.

The question of parametric resonance in a continuous medium arose in the 1950s in connection with the work of Bloembergen, Damon and Wang^[3] on ferromagnetic resonance at high power levels.

This work lead to the discovery of "additional" (as compared with the case of small amplitudes) absorption of the energy of uniform precession of magnetization, which has clearly defined amplitude threshold.

Suhl^[4] explained this phenomenon as parametric instability of uniform precession to the excitation of a pair of spin waves with frequencies ω_1, ω_2 and wave vectors k_1 and k_2 . He was the first to formulate the conditions for parametric resonance in a continuous medium. In contrast to the previous condition for parametric resonance for an oscillator, namely, $n\omega_p = 2\omega$, the new conditions take the form

$$n\omega_p = \omega_1 + \omega_2, \quad k_1 + k_2 = 0; \quad (1.1)$$

where ω_p is the uniform precession frequency. Since $k_2 = -k_1$, parametric instability results in the creation of a pair of waves with equal and opposite wave vectors. The number n determines the "order" of the instability.

In 1960, Morgenthaler^[5] and, independently, Schlömann, Green, and Milano^[6] predicted (and this was subsequently confirmed experimentally) the phenomenon of "parallel pumping," i.e., the parametric excitation of spin waves by an alternating magnetic field with polarization parallel to the direction of magnetization. In the course of the following years, parallel excitation became one of the main methods of generation of spin waves in ferromagnets.

Studies of parametric instabilities in plasmas and in nonlinear optics began in the 1960s. In 1962, Oraevskii and Sagdeev^[7] used the example of Langmuir and ion-acoustic waves in plasma to develop the theory of decay instability (first order instability) of finite-amplitude monochromatic waves in a nonlinear medium. For an initial wave of frequency ω and wave vector k , this instability leads to the excitation of a pair of waves, the frequencies and wave vectors of which satisfy the conditions

$$\omega = \omega_1 + \omega_2, \quad k = k_1 + k_2. \quad (1.2)$$

These conditions are an obvious generalization of (1.1) for $n = 1$ in the case of first-order parametric instability. This instability can be looked upon as the coherent decay of the initial quanta (k, ω) into pairs of quanta ($k_1\omega_1, k_2\omega_2$), and the relationships given by (1.2) can be regarded as the conservation laws for this decay.

Stimulated Raman scattering (SRS) and stimulated Mandel'shtam-Brillouin scattering (SMBS) were predicted and confirmed experimentally in optics at more or less the same time. These phenomena are in fact the decay instabilities of an electromagnetic wave, leading to the excitation of another electromagnetic wave and optical (in the case of SRS) or acoustic (in the case of SMBS) phonons (see for example^[8]). The conditions given by (1.2) have been referred to in nonlinear optics as the synchronism or locking conditions.

A substantial number of papers on parametric instabilities in continuous media have appeared in the literature in the course of the subsequent years (see the review^[9]). Published investigations have covered, for example, the parametric instability of a uniform electric field in plasma^[10], the second-order decay instability of finite-amplitude waves^[11], and the instability of waves on the surface of a liquid^[12-14]. The linear theory of parametric instabilities in uniform continuous media can now be regarded as essentially complete.

The situation is quite different in the case of the nonlinear theory. Wave turbulence appears as a result of the development of parametric instability in a continuous medium (if the linear dimensions of the system are sufficiently large in comparison with the wavelength of the excited waves). However, the character of this turbulence is strongly dependent upon each specific situation, the form of the dispersion relation, and the nonlinear and dissipative properties of the medium, which are quite different in different cases, so that one can hardly hope to develop a general theory of wave turbulence. Quite frequently, for example, in SRS or SMBS of electromagnetic waves entering a half-space, the turbulence cannot be looked upon as statistically homogeneous, and this introduces an additional complication.

Nevertheless, it is possible to isolate a class of problems in parametric turbulence for which a general approach can be employed. This class includes cases where the excitation is produced by a spatially homogeneous field $k = 0$ or a wave with a long wavelength $k \ll k_1, k_2$, so that turbulence may be looked upon as statistically homogeneous. A further requirement is that the dispersion relations for the medium should exclude first-order decay processes (1.2) for parametrically excited waves. It is precisely this situation which occurs in most experiments on the parametric excitation of spin waves in ferromagnets. It is important to note that these experiments belong to a class of the "purest" experiments in the physics of nonlinear waves because of their relative simplicity (in comparison, for example, with plasma or nonlinear-optics experiments), and the high quality of the ferromagnetic single crystals employed. A particularly suitable medium for experimental study is the YIG crystal [the garnet $(Y_3Fe_5O_{12})^{[15,16]}$] which has many unique properties, including a completely ordered magnetic structure, high degree of uniformity, record value of the acoustic Q factor (10^7 at 10^6 Hz), and weak spin-wave damping. Most of the experimental data described in this review relate to YIG.

Experimental data on spin turbulence have been accumulating since the beginning of the 1960s. First models were introduced at about the same time and were designed, above all, to account for the mechanism which restricts the growth in the amplitude of unstable spin waves.

The first step in this direction was made in Sühl's paper^[4] where it was shown that the principal amplitude-restricting mechanism in the case of excitation of spin waves by homogeneous precession of magnetization is the reaction of these waves on the pump, which leads to the "freezing" of the amplitude at the threshold level. However, attempts to explain the phenomena observed in the case of parallel pumping have encountered considerable difficulties. The use of the various methods of restraining parametric instability, which were traditional for parametric resonance, in systems with a small number of degrees of freedom (nonlinear damping and nonlinear frequency detuning) has turned out to be inadequate. In most cases nonlinear damping is too weak, and too sensitive to the effect of the constant magnetic field, to explain the observed spin-wave level, whilst nonlinear frequency detuning does not, in general, restrict parametric resonance in a continuous medium, since it is always possible (whatever the amplitude) to find waves whose renormalized frequencies satisfy the resonance conditions exactly.

An important step toward an understanding of spin turbulence was made by Schrömann^[17], who drew attention to the fact that the nonlinear interaction between the parametrically excited waves must be taken into account, and suggested that the main contribution to this interaction is due to nonlinear processes which satisfy the conditions

$$\omega_{\mathbf{k}} + \omega_{-\mathbf{k}} = \omega_{\mathbf{k}'} + \omega_{-\mathbf{k}'} \quad (1.3)$$

and do not take the waves out of parametric resonance. Bierlein and Richards^[18] then showed that this type of interaction must be taken into account if one is to explain the observed frequency doubling for spin waves.

In 1969, the present authors showed^[19] that processes of the type described by (1.3) conserve phase correlation within each parametrically excited pair of waves with opposite wave vectors, and lead to a self-consistent change in the resultant phase of the waves in each pair. This change in the resultant phase leads to a weakening of the coupling between the spin waves and the pump and, in the final analysis, to a restriction on their amplitude. The excited waves are then precisely those for which the renormalized frequencies satisfy exactly the parametric resonance condition. This "phase" mechanism of amplitude limitation is specific for continuous media and is realized in pure form only in systems with very large linear dimensions (in comparison with the wavelength). It is the principal mechanism limiting the amplitudes of spin waves in the case of parallel pumping.

Processes of the form described by (1.3) together with the necessary phase relationships are conveniently investigated by diagonalizing the Hamiltonian for the wave interaction, which is analogous to the BCS approximation in the theory of superconductivity. The theory based on this diagonalization procedure^[20] was subsequently called the S theory. This theory and its generalizations subsequently resulted in considerable progress in the study of spin-wave turbulence. It provided a qualitative explanation of many of the observed effects, and gave satisfactory quantitative agreement with experimental data^[21-24].

A serious test for S theory was the question of the auto-oscillation of magnetization during the parametric excitation of spin waves. As far back as 1961 Hartwick, Peressini, and Weiss^[25] discovered that parallel pumping lead, under certain conditions, to the establishment not of a steady state but to oscillations in the magnetization about its mean value. During the subsequent years these auto-oscillations were intensively investigated and it was found that their properties, i.e., their amplitude and spectral composition, were very sensitive to all the experimental parameters, namely, the pump power, the magnetic field, the shape and size of the specimens, and so on, and this substantially impeded the interpretation of these results. A particularly strange feature was the sensitivity to the crystallographic orientation of the magnetization of YIG (a crystal which exhibits weak cubic anisotropy). The intensity of the auto-oscillations when the magnetization lay along the $\langle 111 \rangle$ axis exceeded by a factor of 100 their intensity when the magnetization lay along the $\langle 100 \rangle$ axis. Various mechanisms were then introduced to explain the origin of the auto-oscillations (see Sec. 5 of the present review), but none of them succeeded in satisfactorily explaining this phenomenon.

The S theory attributes auto-oscillations in magneti-

zation to the instability of collective oscillations of a system of parametric spin waves. They can be treated as "secondary turbulence" or "second-sound turbulence" against the background of the stationary state of the parametrically excited waves. This has led to an explanation of some of the more important properties of the auto-oscillations and, in particular, their giant anisotropy in cubic ferromagnets^[26].

When collective oscillations are stable, and do not lead to auto-oscillations, they can be excited by combinational resonance between the pump and a weak signal of similar frequency. An experiment of this kind has been carried out^[27] and demonstrated the reality of the collective oscillations. On the whole, the S theory and its consequences have enabled us to understand in general terms, the properties of spin turbulence in ferromagnets, although further experiments will undoubtedly reveal new phenomena which will require further improvements of this theory.

As an example of this type of phenomenon we mention the hard excitation of spin waves in ferromagnets, discovered by Le Gall, Lemire and Sere^[28]. This phenomenon was subsequently found in antiferromagnets as well^[29]. The S theory and its experimental verification is the main subject of the present review (Secs. 2-4). Section 5 is devoted to the further development of the S theory and, in particular, to its fundamentals. In the concluding section, we discuss associated topics and possible future developments.

2. PARAMETRIC INSTABILITY IN FERROMAGNETICS

(a) Classical Hamilton formalism for ferromagnets. There are several methods of describing the spin-wave system of ferromagnets. The most highly developed is the method of second quantization, first used by Holstein and Primakoff^[30] to describe the temperature dependence of magnetization near the absolute zero. In the case of parametric excitation of magnons, their occupation numbers turn out to be greater than unity by several orders of magnitude, so that it is natural to use the classical equations of motion for the magnetic-moment density to describe this phenomenon (see, for example,^[31]):

$$\frac{\delta \mathbf{M}}{\delta t} = g \left[\mathbf{M}, \frac{\delta W}{\delta \mathbf{M}} \right], \quad (2.1)$$

where $\delta W / \delta \mathbf{M}$ is the variational derivative of the energy density of the ferromagnet and g is the gyromagnetic ratio. Sühl^[4] was the first to use Eq. (2.1) for the analysis of the parametric excitations of spin waves and the associated nonlinear phenomena. However, the parametric-excitation problem is not peculiar to ferromagnets, and it is desirable to use a general approach, applicable to a broad class of weakly interacting wave systems. The most convenient method for this purpose is the classical Hamilton formalism. This is based on the canonical equations of motion

$$\frac{\partial a(\mathbf{r}, t)}{\partial t} = -i \frac{\delta \mathcal{H}}{\delta a^*}, \quad (2.2)$$

where \mathcal{H} is the Hamiltonian of the medium.

In the case of ferromagnets, direct calculations show^[32] that Eq. (2.1) assumes the canonical form given by (2.2) when the following substitutions are introduced:

$$M_x + iM_y = \sqrt{2gM} a \sqrt{1 - g \frac{aa^*}{M}}, \quad M_z = M - gaa^*. \quad (2.3)$$

In terms of the variables a and a^* the energy of the ferromagnet is a function of the Hamiltonian. The trans-

formations defined by (2.3) are the classical analog of the Holstein-Primakoff transformation.^[30] They were first used by Schlömann^[17] in the present context.

In a spatially homogeneous medium, the structure of the Hamiltonian can be substantially simplified by making use of the plane-wave representation

$$a_{\mathbf{k}} = \int a(\mathbf{r}) e^{-i\mathbf{k}\cdot\mathbf{r}} d\mathbf{r}. \quad (2.4)$$

Since in the case of parametric excitation of spin waves the deviation of the magnetic moment from equilibrium is small ($g|a|^2 \ll M$), we can expand the Hamiltonian into a series in powers of $a_{\mathbf{k}}$ and $a_{\mathbf{k}}^*$. The quadratic part of the Hamiltonian \mathcal{H} is diagonal in \mathbf{k} :

$$\mathcal{H}^{(2)} = \sum_{\mathbf{k}} \left\{ A_{\mathbf{k}} a_{\mathbf{k}} a_{\mathbf{k}}^* + \frac{1}{2} [B_{\mathbf{k}} a_{\mathbf{k}}^* a_{-\mathbf{k}} + B_{\mathbf{k}}^* a_{\mathbf{k}} a_{-\mathbf{k}}] \right\}.$$

For example, in a cubic ferromagnet magnetized along the $\langle 111 \rangle$ or $\langle 100 \rangle$ axis,

$$\begin{aligned} A_{\mathbf{k}} &= gH - \omega_M N_z + \omega_{\text{ex}} (ak)^2 + |B_{\mathbf{k}}| + \alpha \omega_a, \\ B_{\mathbf{k}} &= \frac{1}{2} \omega_M \sin^2 \theta e^{2i\varphi}, \\ \alpha &= \begin{cases} -1, & \mathbf{M} \parallel \langle 100 \rangle, \\ \frac{2}{3}, & \mathbf{M} \parallel \langle 111 \rangle; \end{cases} \end{aligned}$$

where $\omega_M = 4\pi gM$, H is the magnetic field, ω_{ex} is the "exchange frequency" ($\hbar\omega_{\text{ex}} \approx kT_C$), ω_a/g is the crystallographic anisotropy field, θ and φ are the polar and azimuthal angles defining the vector \mathbf{k} in a spherical coordinate system whose z axis lies along \mathbf{M} , and N_z is the demagnetization factor.

The problem can be simplified still further by using the canonical transformation from circular variables $a_{\mathbf{k}}$ to elliptic variables $b_{\mathbf{k}}$:

$$a_{\mathbf{k}} = u_{\mathbf{k}} b_{\mathbf{k}} + v_{\mathbf{k}} b_{-\mathbf{k}}^*, \quad |u_{\mathbf{k}}|^2 - |v_{\mathbf{k}}|^2 = 1,$$

which must be chosen so that the quadratic part of the Hamiltonian becomes diagonal

$$u_{\mathbf{k}} = \sqrt{\frac{A_{\mathbf{k}} + \omega_{\mathbf{k}}}{2\omega_{\mathbf{k}}}}, \quad v_{\mathbf{k}} = -\frac{B_{\mathbf{k}}}{|B_{\mathbf{k}}|} \sqrt{\frac{A_{\mathbf{k}} - \omega_{\mathbf{k}}}{2\omega_{\mathbf{k}}}},$$

where $\omega_{\mathbf{k}} = \sqrt{(A_{\mathbf{k}} - |B_{\mathbf{k}}|^2)^{1/2}}$ is the dispersion relation for the spin waves. In terms of these variables

$$\mathcal{H}^{(2)} = \sum_{\mathbf{k}} \omega_{\mathbf{k}} b_{\mathbf{k}} b_{\mathbf{k}}^*. \quad (2.5)$$

For cubic ferromagnets

$$\omega_{\mathbf{k}}^2 = \left[gH - \omega_M N_z + \omega_{\text{ex}} (ak)^2 + \alpha \omega_a + \omega_M \frac{\sin^2 \theta}{2} \right]^2 - \frac{\omega_M^2 \sin^4 \theta}{4}. \quad (2.6)$$

This transformation is possible if $|A_{\mathbf{k}}| > |B_{\mathbf{k}}|$, i.e., $H > 4\pi N_z M$. In the opposite case, $\omega^2(0) < 0$ and the ferromagnet is unstable against the appearance of domain structure.

It is obvious that the variables $b_{\mathbf{k}}$ satisfy the Hamilton equation

$$\dot{b}_{\mathbf{k}} = -i \frac{\delta \mathcal{H}}{\delta b_{\mathbf{k}}^*}.$$

These variables are the normal variables of the linear theory, and are particularly convenient for nonlinear problems. Specifically "linear" difficulties associated with this model of the medium are overcome in the course of the search for the variables $b_{\mathbf{k}}$. In terms of these variables, the linearization of the equations in motion is a fairly trivial task:

$$b_{\mathbf{k}} + i\omega_{\mathbf{k}} b_{\mathbf{k}} = 0.$$

All the "linear" information which is essential for investigating nonlinear problems is contained in the dispersion relation for the waves. All the additional information about the interaction between the waves is contained in the remaining coefficients of the expansion of \mathcal{H} in powers of $b_{\mathbf{k}}$:

$$\mathcal{H} = \mathcal{H}^{(2)} + \mathcal{H}^{(3)} + \mathcal{H}^{(4)} + \dots \quad (2.7)$$

The Hamiltonian $\mathcal{H}^{(3)}$ describes the three-wave processes:

$$\begin{aligned} \mathcal{H}^{(3)} = \sum_{1, 2, 3} (V_{1, 23}^* b_1^* b_2 b_3 + \text{c.c.}) \Delta(\mathbf{k}_1 - \mathbf{k}_2 - \mathbf{k}_3) \\ + \frac{1}{3} \sum_{1, 2, 3} (U_{123}^* b_1 b_2 b_3 + \text{c.c.}) \Delta(\mathbf{k}_1 + \mathbf{k}_2 + \mathbf{k}_3), \end{aligned} \quad (2.8)$$

whilst the Hamiltonian $\mathcal{H}^{(4)}$ describes the four-wave processes:

$$\mathcal{H}^{(4)} = \frac{1}{2} \sum_{12, 34} W_{12, 34} b_1^* b_2^* b_3 b_4 \Delta(\mathbf{k}_1 + \mathbf{k}_2 - \mathbf{k}_3 - \mathbf{k}_4); \quad (2.9)$$

where $b_1 = b_{\mathbf{k}_1}$ and so on; $V_{1, 23} = V(\mathbf{k}_1, \mathbf{k}_2, \mathbf{k}_3)$. The coefficients $V_{1, 23}$, U_{123} , $W_{12, 34}$ are symmetric with respect to the interchange of the subscripts on the same side of the comma. Since the Hamiltonian is Hermitian, we also have

$$W_{12, 34} = W_{34, 12}. \quad (2.10)$$

The physical significance of each of the terms in the Hamiltonian can readily be understood by recalling that the canonical variables $b_{\mathbf{k}}$ and $b_{\mathbf{k}}^*$ are the classical analogs of the Bose operators. For example, the term proportional to $V_{1, 23}$ describes, together with its complex conjugate, the interaction of three-waves of the form given by (1.2). Henceforth we shall assume, unless stated to the contrary, that processes of this type are forbidden by the form of the dispersion law in the region of \mathbf{k} space in which we are interested.

When an external energy source is present, i.e., the pump field $h(t)$, the Zeeman component $M \cdot h$ is added to the energy of the ferromagnet. The Hamiltonian \mathcal{H}_p corresponding to this interaction can also be expanded in powers of $b_{\mathbf{k}}$:

$$\mathcal{H}_p = \mathcal{H}_p^{(1)} + \mathcal{H}_p^{(2)} + \dots$$

The first term is

$$\mathcal{H}_p^{(1)} = U(h_x + ih_y) b_0 + \text{c.c.} \quad (2.11)$$

and describes the well-known phenomenon of ferromagnetic resonance which involves the excitation of homogeneous precession of magnetization with complex amplitude b_0 by the transverse magnetic field. The next term in the expansion, $\mathcal{H}_p^{(2)}$, is of the greatest interest to us and describes the parametric excitation of spin waves by the longitudinal magnetic field (parallel pumping):

$$\mathcal{H}_p^{(2)} = \frac{1}{2} \sum_{\mathbf{k}} \mathcal{H}_{p\mathbf{k}} = \frac{1}{2} \sum_{\mathbf{k}} (h(t) V_{\mathbf{k}} b_{\mathbf{k}}^* b_{-\mathbf{k}} + \text{c.c.}), \quad h = \frac{hM}{|M|}. \quad (2.12)$$

The mechanism responsible for the excitation of spin waves by an alternating magnetic field parallel to the magnetization can be understood in terms of simple geometric ideas. Because of the dipole-dipole interaction and the crystallographic anisotropy, the magnetization precesses at each point over an elliptic cone. Since the length of the vector \mathbf{M} remains constant, the base of the cone is not a plane, so that we have an alternating longitudinal component (the z component) of the vector \mathbf{M} which varies at twice the precession frequency. It is clear that these oscillations can be excited by a

magnetic field of the necessary frequency, polarized along the z axis.

In corpuscular language, the Hamiltonian given by (2.12) describes the decay of an external-field quantum (with zero wave vector and energy $\hbar\omega_p$) into two magnons with wave vectors \mathbf{k} and $-\mathbf{k}$ and equal energies $\hbar\omega_{\mathbf{k}} = \hbar\omega_{-\mathbf{k}} = 1/2\hbar\omega_p$. We have omitted from (2.12) terms $\sim h(t)b_{\mathbf{k}}b_{-\mathbf{k}}^*$ for which the laws of conservation of energy and momentum are not satisfied.

The parametric excitation of spin waves by homogeneous precession of magnetization, which is described by terms of the form $b_{\mathbf{k}}b_{\mathbf{k}}^*b_{-\mathbf{k}}^*$ and $b_{\mathbf{k}}^*b_{-\mathbf{k}}^*$ (first and second order Suhl processes), is included in the Hamiltonians $\mathcal{H}^{(3)}$ and $\mathcal{H}^{(4)}$. The next expansion terms are of the form $hb_{\mathbf{k}}^*b_{\mathbf{k}}^*b_{-\mathbf{k}}^*$, and so on. They describe explosive spin-wave instabilities which are not of interest to us.

(b) The equations of motion. Consider a ferromagnet placed in an alternating magnetic field $h(t) = he^{-i\omega_pt}$ which is polarized along the direction of magnetization. In this case, homogeneous precession is not excited and the Hamiltonian for the system is of the form

$$\mathcal{H} = \sum_{\mathbf{k}} \omega_{\mathbf{k}} b_{\mathbf{k}} b_{\mathbf{k}}^* + \frac{1}{2} \sum_{\mathbf{k}} (hV_{\mathbf{k}} e^{-i\omega_pt} b_{\mathbf{k}}^* b_{-\mathbf{k}}^* + c.c.) + \mathcal{H}_{int}, \quad (2.13)$$

where $\mathcal{H}_{int} = \mathcal{H}^{(3)} + \mathcal{H}^{(4)}$. Since all parametric waves have close or equal frequencies ($\omega_{\mathbf{k}} \approx 1/2\omega_p$), we can simplify the interaction Hamiltonian \mathcal{H}_{int} by retaining in it only the four-wave terms describing the interaction of waves with conservation laws in the form

$$\omega_{\mathbf{k}_1} + \omega_{\mathbf{k}_2} = \omega_{\mathbf{k}_1+\mathbf{x}} + \omega_{\mathbf{k}_2-\mathbf{x}}. \quad (2.14)$$

The latter do not, however, mean that the three-wave Hamiltonian can be ignored altogether. Its matrix elements are large in comparison with the four-wave case and, therefore, in general their contribution to the amplitude for the four-wave processes must be taken into account in the second order of perturbation theory. This leads to the renormalization of the matrix elements for the four-wave Hamiltonian:

$$W_{12,34} \rightarrow T_{12,34} = W_{12,34} + \text{terms of the order of } |V|^2/\omega_p$$

(see, for example, [32]). For cubic ferromagnets, both contributions to the coefficients $T_{12,34}$ are of the same order of magnitude [22]. Therefore, the Hamiltonian describing the parametric interaction between the waves must be chosen in the form

$$\mathcal{H}_{int} = \frac{1}{2} \sum_{12,34} T_{12,34} b_1^* b_2^* b_3 b_4 \Delta(\mathbf{k}_1 + \mathbf{k}_2 - \mathbf{k}_3 - \mathbf{k}_4). \quad (2.15)$$

It is of course necessary to take into account the interaction between the parametric waves and the reservoir of the remaining spin waves and phonons. This interaction leads to the damping of the parametric waves, which is usually taken into account phenomenologically by introducing a dissipative term into the canonical equations of motion:

$$\dot{b}_{\mathbf{k}} + \gamma_{\mathbf{k}} b_{\mathbf{k}} = -i \frac{\delta \mathcal{H}}{\delta b_{\mathbf{k}}^*}. \quad (2.16)$$

There may be some doubt as to the validity of this procedure for the description of coherent wave systems in which phase relationships are significant. This procedure was justified in [33] for parametric waves with the aid of the diagram technique, and it was shown that the damping rate $\gamma_{\mathbf{k}}$ in (2.16) can be calculated from the usual kinetic equations. This does not apply, however,

when the wave damping is due to scattering by inhomogeneities.^[34]

Using the explicit form of the Hamiltonian given by (2.13), with \mathcal{H}_{int} given by (2.15), we can write the dynamic equations (2.16) in the form

$$\left(\frac{d}{dt} + \gamma_{\mathbf{k}} + i\omega_{\mathbf{k}} \right) b_{\mathbf{k}} + ihV_{\mathbf{k}} e^{-i\omega_pt} b_{-\mathbf{k}}^* \\ = - \sum_{2,34} T_{\mathbf{k}_1 \mathbf{k}_1 \mathbf{k}_2 \mathbf{k}_3} b_{\mathbf{k}_1}^* b_{\mathbf{k}_2}^* b_{\mathbf{k}_3} \Delta(\mathbf{k}_1 + \mathbf{k}_2 - \mathbf{k}_3 - \mathbf{k}_4). \quad (2.17)$$

These equations form the starting point for the analysis of the behavior of spin waves beyond the parametric excitation threshold.

(c) Excitation threshold and amplitude-limiting mechanisms. The parametric excitation threshold can be calculated directly from (2.17). In the linear approximation, these equations split into independent pairs of equations, and when the "fast" dependence on time

$$c_{\mathbf{k}}(t) = b_{\mathbf{k}}(t) e^{\frac{i\omega_pt}{2}} \quad (2.18)$$

is eliminated, they assume the form

$$\left[\frac{d}{dt} + \gamma_{\mathbf{k}} + i \left(\omega_{\mathbf{k}} - \frac{\omega_p}{2} \right) \right] c_{\mathbf{k}} + ihV_{\mathbf{k}} c_{-\mathbf{k}}^* = 0, \\ i(hV_{\mathbf{k}})^* c_{\mathbf{k}} + \left[\frac{d}{dt} + \gamma_{\mathbf{k}} - i \left(\omega_{\mathbf{k}} - \frac{\omega_p}{2} \right) \right] c_{-\mathbf{k}}^* = 0. \quad (2.19)$$

Assuming that $c_{\mathbf{k}}, c_{-\mathbf{k}} \sim \nu_{\mathbf{k}}$ we have

$$V_{\mathbf{k}} = -\gamma_{\mathbf{k}} + \left[|hV_{\mathbf{k}}|^2 - (\omega_{\mathbf{k}} - \frac{\omega_p}{2})^2 \right]^{1/2}. \quad (2.20)$$

The minimum threshold corresponding to parametric resonance

$$2\omega_{\mathbf{k}} = \omega_p, \quad (2.21)$$

is determined by the condition

$$|hV_{\mathbf{k}}| = \gamma_{\mathbf{k}}, \quad (2.22)$$

which has the simple interpretation of an energy balance condition. In fact, the energy flux W_+ which is transferred from the pump to the pair of waves $\pm \mathbf{k}$ is given by

$$W_+ = -\frac{\partial \mathcal{H}_{pk}}{\partial t} = i\omega_p (hV_{\mathbf{k}} c_{\mathbf{k}}^* c_{-\mathbf{k}} - c.c.) \\ = 2|hV_{\mathbf{k}}| \omega_p |c_{\mathbf{k}}|^2 \sin(\tilde{\psi}_{\mathbf{k}} - \psi_{\mathbf{k}});$$

where $c_{\mathbf{k}} = |c_{\mathbf{k}}|e^{i\varphi_{\mathbf{k}}}$, $\psi_{\mathbf{k}} = \varphi_{\mathbf{k}} + \varphi_{-\mathbf{k}}$ is the phase of the pair, and $\tilde{\psi}_{\mathbf{k}} = \arg(hV_{\mathbf{k}})$. On the other hand, the energy dissipated by the pair per unit time is given by

$$W_- = 2\gamma_{\mathbf{k}} (\omega_{\mathbf{k}} |c_{\mathbf{k}}|^2 + \omega_{-\mathbf{k}} |c_{\mathbf{k}}|^2) = 2\omega_p \gamma_{\mathbf{k}} |c_{\mathbf{k}}|^2.$$

At the threshold $W_+ = W_-$. The maximum energy flux and the lowest instability threshold is obtained for the pair with the most convenient phase relationship

$$\psi_{\mathbf{k}} = \tilde{\psi}_{\mathbf{k}} + \frac{\pi}{2}. \quad (2.24)$$

We then again obtain equation (2.22) for the threshold.

The parametric resonance condition can obviously be simultaneously satisfied for a large number of pairs whose wave vectors lie on the surface (2.21). The minimum excitation threshold h_1 is obtained for pairs for which the ratio $\gamma_{\mathbf{k}}/|V_{\mathbf{k}}|$ is a minimum:

$$h_1 = \min \frac{\gamma_{\mathbf{k}}}{|V_{\mathbf{k}}|}. \quad (2.25)$$

For example, in the case of isotropic ferromagnets^[5, 6]

$$V_{\mathbf{k}} = V \sin^2 \theta \cdot e^{2i\varphi} \quad (2.26)$$

(the angles θ and φ are, as before, the azimuthal and

polar angles in \mathbf{k} space), and when $\gamma_{\mathbf{k}} = \gamma$ the first to be excited are the pairs with $\theta = \pi/2$, i.e., those on the "equator" of the resonance surface. When $|hV_{\mathbf{k}}| > \gamma_{\mathbf{k}}$, the amplitude of the pairs begins to increase exponentially with growth rate (2.20). In particular

$$c_{\mathbf{k}}(t) = c_{\mathbf{k}} \exp\left(V_{\mathbf{k}} t - i \frac{\psi_{\mathbf{k}}}{2}\right),$$

$$c_{-\mathbf{k}}(t) = c_{\mathbf{k}}^* \exp\left(V_{\mathbf{k}} t + i \frac{\psi_{\mathbf{k}}}{2}\right),$$

and it follows from (2.19) that

$$\cos(\psi_{\mathbf{k}} - \tilde{\psi}_{\mathbf{k}}) = \frac{2\omega_{\mathbf{k}} - \omega_p}{2|hV_{\mathbf{k}}|}. \quad (2.27)$$

This means that, during the linear stage of parametric instability, a definite relationship is established between the phases of the waves in a pair. In particular, the phase relations given by (2.24) are satisfied in the case of the parametric resonance (2.21). The phase correlation of waves with equal and opposite wave vectors can be referred to as "pairing" by analogy with superconductivity. However, in contrast to superconductivity, the physical reason responsible for wave pairing is the presence of the pump which picks out pairs of waves out of the initial phase chaos for which the instability growth rate is a maximum. We shall show later that phase correlation is complete during the nonlinear stage of instability development. This means that although the quantity $c_{\mathbf{k}} c_{-\mathbf{k}}$ is random, the quantity $c_{\mathbf{k}} c_{-\mathbf{k}}$ is dynamic, and

$$\langle c_{\mathbf{k}} c_{-\mathbf{k}} \rangle = c_{\mathbf{k}} c_{-\mathbf{k}}, \quad \langle \psi_{\mathbf{k}} \rangle = \psi_{\mathbf{k}}.$$

Let us now consider possible nonlinear mechanisms which limit parametric instability. The simplest mechanism of this kind is nonlinear damping, i.e., the dependence of $\gamma_{\mathbf{k}}$ on the squares of the amplitude of the parametric waves $|c_{\mathbf{k}}|^2$ [35, 36].

$$\gamma_{\mathbf{k}} = \gamma_0 + \eta \sum_{\mathbf{k}'} |c_{\mathbf{k}'}|^2.$$

The stationary wave amplitudes are given by the well-known energy balance condition $hV_{\mathbf{k}} = \gamma_{\mathbf{k}}$. We shall choose the following simple dependence for qualitative analysis:

$$\gamma_{\mathbf{k}} = \gamma_{\mathbf{k}}(0) + \gamma_{\mathbf{k}}^{nl} (|c_{\mathbf{k}}|^2).$$

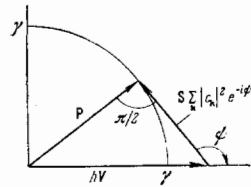
In that case,

$$\sum_{\mathbf{k}'} |c_{\mathbf{k}'}|^2 = \frac{hV - \gamma_0}{\eta} = \frac{V}{\eta} (h - h_0); \quad (2.28)$$

and the phases $\psi_{\mathbf{k}}$ are found from the condition of parametric resonance (2.21), i.e., they are shifted by $1/2\pi$ relative to the pump phase, in accordance with (2.24).

Unfortunately, the simple nonlinear damping mechanism is not adequate in most cases for the explanation of the observed level of spin waves (see Sec. 3 for further details). Other mechanisms may be based on the deviation of the phase of the excited spin waves from the optimum phase for which $\delta\psi_{\mathbf{k}} = \psi_{\mathbf{k}} - \tilde{\psi}_{\mathbf{k}}$ and $\sin \delta\psi_{\mathbf{k}} = 1$. This is essentially the mechanism put forward by Monosov [37] who assumed that auto-oscillations of magnetization play an important role in limiting the spin-wave amplitude, and are frequently observed experimentally. If the auto-oscillations develop against a background of a state with $\sin \delta\psi_{\mathbf{k}} = 1$, they lead to a periodic or quasi-periodic variation in the angle $\delta\psi_{\mathbf{k}}$ and, on the average, reduce $\sin \delta\psi_{\mathbf{k}}$ and with it the energy flux from the pump to the spin-wave system. In actual fact, the auto-oscillations do not appear in many cases. However, even when they do appear, the mean value about which the oscillations with phase $\psi_{\mathbf{k}}$ take place is different

FIG. 1. Complex plane of the pump vectors: hV —external pump, $S \sum_{\mathbf{k}} |\mathbf{c}_{\mathbf{k}}|^2 e^{-i\varphi_{\mathbf{k}}}$ —reaction field of the system of pairs, P —self-consistent pump.



from $1/2\pi$, and the auto-oscillations have no substantial effect on the spin-wave amplitudes [23, 38].

The deviation of $\psi_{\mathbf{k}}$ from $1/2\pi$ and the restriction on the spin-wave amplitude are due to the interaction between the spin waves. The phase correlation which is always present in a system of parametrically excited waves ensures that, even when the phases of the individual spin waves are stochastic, the Hamiltonian describing their interaction contains a term which leads to the appearance of an "effective pump." This term can be taken into account by introducing the following substitutions in the linearized equations:

$$hV_{\mathbf{k}'} \rightarrow p_{\mathbf{k}} = hV_{\mathbf{k}} + \sum_{\mathbf{k}'} S_{\mathbf{k}\mathbf{k}'} c_{\mathbf{k}'} c_{-\mathbf{k}'}, \quad (2.29)$$

where $S_{\mathbf{k}\mathbf{k}'} = T_{\mathbf{k}-\mathbf{k}; \mathbf{k}'-\mathbf{k}'}$. In the simplest case, where $V_{\mathbf{k}} = V$, $\psi_{\mathbf{k}} = 0$, and $S_{\mathbf{k}\mathbf{k}'} = S$, symmetry considerations show that the phases of all the pairs are equal, i.e., $\psi_{\mathbf{k}} = \psi$ and

$$P = hV + S \sum_{\mathbf{k}} |c_{\mathbf{k}}|^2 \exp(-i\psi). \quad (2.30)$$

This equation is conveniently represented graphically on the complex plane of the pump vectors (Fig. 1). It is then important to remember that, in the steady state, we have the excitation of waves which are in resonance with the resultant pump P , i.e., the vector P in Fig. 1 should be perpendicular to the vector $S \sum_{\mathbf{k}} |c_{\mathbf{k}}|^2 \exp(-i\psi)$. From the Pythagoras theorem,

$$(hV)^2 = |P|^2 + S^2 \left(\sum_{\mathbf{k}} |c_{\mathbf{k}}|^2 \right)^2 \quad (2.31)$$

and the energy balance condition $|P| = \gamma$ it follows that the total pair amplitude is

$$\sum_{\mathbf{k}} |c_{\mathbf{k}}|^2 = \frac{\sqrt{(hV)^2 - \gamma^2}}{|S|}.$$

The phase ψ can also be easily determined from Fig. 1; namely

$$\cos \psi = -S \frac{\sum_{\mathbf{k}} |c_{\mathbf{k}}|^2}{hV}, \quad \sin \psi = \frac{\gamma}{hV}. \quad (2.32)$$

If we compare the second equation in (2.32) with the energy balance condition (2.22) for noninteracting waves, we see that wave pairing and the resulting four-wave interaction lead to the violation of the phase matching between the pairs and the external pump ($\sin \psi < 1$), i.e., to a reduction in the energy flux into the system.

This limiting mechanism, which may be referred to as the phase mechanism, plays a determining role during parametric excitation of waves. We note that in previous analyses it was assumed that the parametric resonance conditions were satisfied exactly for all excited-wave amplitudes. When wave frequency shift due to the nonlinearity is present, this is possible only for a continuous spectrum of the spin-wave system, and therefore, the phase mechanism is realized in pure form only in infinite media.

(d) Nonlinear susceptibilities and methods of measuring them. The most widely used method of experimental investigation of parametric excitation of spin waves is

based on the absorption of pump energy by the waves.

We shall define the high-frequency nonlinear susceptibility of a ferromagnet in the usual way, i.e.,

$$M_z(\omega_p) = \chi h, \quad \chi = \chi' + i\chi''.$$

The imaginary part of the susceptibility χ'' , determines the absorbed power:

$$W = \frac{\omega_p}{2} \chi'' h^2.$$

If we use (2.23) to determine the energy flowing into the specimen from the surrounding pump field, we obtain

$$\chi'' = \frac{2}{h} \sum_k |V_k| |c_k|^2 \sin(\tilde{\psi}_k - \psi_k). \quad (2.33)$$

A similar expression is obtained for the real part of the susceptibility:

$$\chi' = -\frac{2}{h} \sum_k |V_k| |c_k|^2 \cos(\tilde{\psi}_k - \psi_k). \quad (2.34)$$

The behavior of the real and imaginary parts of the susceptibility beyond the threshold is very dependent on the amplitude-limiting mechanism. Thus, for the nonlinear damping mechanism, we have from (2.24) and (2.28),

$$\chi' = 0, \quad \chi'' = \frac{2V^2}{\eta} \frac{h-h_1}{h}, \quad (2.35)$$

and for the phase mechanism, we have from (2.31) and (2.32),

$$\chi' = \frac{2V^2}{S} \frac{h^2 - h_1^2}{h^2}, \quad \chi'' = \frac{2V^2}{|S|} \frac{h_1 \sqrt{h^2 - h_1^2}}{h^2}. \quad (2.36)$$

Figure 2 shows graphs of the functions $\chi'(h^2)$ and $\chi''(h^2)$ for both cases. The fundamental difference between the dissipative and phase mechanisms can be seen in the behavior of χ' ($\chi' = 0$ for the dissipative and $\chi' \sim \chi''$ for the phase mechanisms). The experimental data, which we shall review in detail in the next section, show that the real part of the susceptibility, χ' , is nonzero and can be of the order of or even greater than χ'' . These facts tend to support the phase mechanism of amplitude limitation.

Measurements of the magnetic susceptibility in the microwave band are usually based on the reaction of the high-Q electromagnetic resonator to changes in the state of the specimen which it contains. The resulting change in Q determines the imaginary part of the susceptibility, χ'' , and the change in the characteristic frequency yields the real part χ' . When compared with standard methods used in magnetic-resonance experiments, the techniques used for measuring the nonlinear susceptibilities in the case of parallel pumping which have a number of specific features. They involve the use of pulsed microwave oscillators, a broad range of fields in which energy absorption is observed, and the fact that χ' and χ'' depend on the pump power. The last fact means that the generator power is not a good measure of the pump-field amplitude. The field in the resonator is more conveniently determined from the power at the

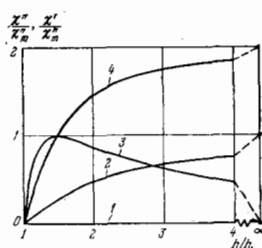


FIG. 2. Nonlinear susceptibilities χ' and χ'' as functions of pump amplitude: 1 and 2— χ' and χ'' for the nonlinear damping mechanism, 3 and 4— χ'' and χ' for the phase limiting mechanism.

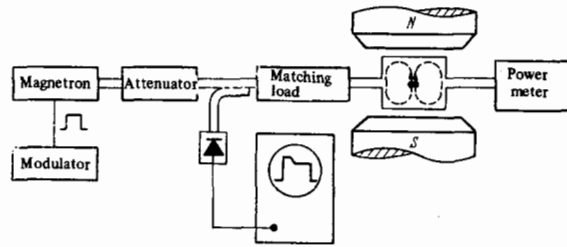


FIG. 3. Schematic illustration of apparatus for the parametric excitation of spin waves.

output of the resonator. This automatically takes into account the reaction of the spin waves on the pump, which is substantial near the threshold even for a small resonator filling factor.

A typical experimental setup used to investigate parallel pumping is illustrated in Fig. 3. The principle of this system is as follows. The undisturbed resonator (below the parametric excitation threshold) is usually matched to a waveguide in such a way that the resonator reflection coefficient is nearly zero. When the spin waves are excited, the Q is reduced and the natural frequency of the resonator ω_0 is shifted. This leads to the appearance of a reflected field which can be used to estimate the magnitudes of χ' and χ'' . The quantity χ'' is related to the reflection coefficient Γ by the formula

$$\chi'' = \frac{1}{AQ} \frac{|\Gamma|_{\omega=\omega_0}}{1-|\Gamma|_{\omega=\omega_0}},$$

where $A = 2\pi \int_{\text{sp.}} h^2 dV / \int_{\text{res.}} h^2 dV$ is the resonator filling factor. Tuning to resonance ($\omega = \omega_0$) is achieved by a small change in the oscillator frequency (or the natural frequency of the resonator), using the minimum of the reflection coefficient. The size of this change, $\Delta\omega = \omega - \omega_0$, yields directly the real part of the susceptibility. For a number of reasons, the main of which is the uncertainty in the measured coefficient A , the uncertainty in the absolute values of χ' and χ'' is usually of the order of 20–40%.

Another method of observing parallel pumping was used in [39] and was based on the change in the magnetization during the parametric excitation of spin waves. The change in the magnetization was recorded by a coil in which a voltage proportional to the time derivative of M_z is induced.

We also recall the method of measuring weak, non-equilibrium electromagnetic emission of spin waves at frequencies ω_p or $1/2\omega_p$ reported in [40]. The interesting possibilities of this method insofar as spectral-width studies are concerned have not as yet been realized for parametric waves. Detailed information on the distribution of spin waves in k space could be obtained by studying the scattering of light and of neutrons under the conditions of parallel pumping. The many attempts made in this area [41–43] have not as yet lead to the expected results.

3. THE STATIONARY POST-THRESHOLD STATE. THE S-THEORY AND ITS COMPARISON WITH EXPERIMENT.

(a) Diagonal Hamiltonian and the equations of motion in S theory. We must now consider in greater detail the simplification of the Hamiltonian for the wave interac-

tion, which was noted in the preceding section in connection with the phase mechanism of amplitude limitation. This simplification is analogous to the BCS approximation, and consists in the replacement of the interaction Hamiltonian (2.15) by its diagonal part for the pairs of waves $\pm \mathbf{k}$. In terms of the "slow variables" (2.18), the diagonal Hamiltonian has the form

$$\tilde{\mathcal{H}}_{\text{int}} = \sum_{\mathbf{k}\mathbf{k}'} T_{\mathbf{k}\mathbf{k}'} |c_{\mathbf{k}}|^2 |c_{\mathbf{k}'}|^2 + \frac{1}{2} \sum_{\mathbf{k}\mathbf{k}'} S_{\mathbf{k}\mathbf{k}'} c_{\mathbf{k}}^* c_{\mathbf{k}'}^* c_{\mathbf{k}'} c_{\mathbf{k}}, \quad (3.1)$$

where

$$T_{\mathbf{k}\mathbf{k}'} \equiv T_{\mathbf{k}\mathbf{k}'}, \quad S_{\mathbf{k}\mathbf{k}'} \equiv T_{\mathbf{k}-\mathbf{k}', \mathbf{k}'-\mathbf{k}'} = S_{\mathbf{k}', -\mathbf{k}'} = S_{\mathbf{k}'-\mathbf{k}}^*. \quad (3.2)$$

In the Hamiltonian \mathcal{H}_{int} we have only those terms which either are independent of the phases [the first sum in (3.1)] or depend only on resultant phase $\psi_{\mathbf{k}} = \varphi_{\mathbf{k}} + \varphi_{-\mathbf{k}}$ in the pairs. All the other terms which depend on the individual phases (or more precisely, on the differences $\varphi_{\mathbf{k}} - \varphi_{\mathbf{k}'}$) are omitted.

The physical meaning of the terms retained in (3.1) is clear from a consideration of the equations of motion for the amplitudes $c_{\mathbf{k}}$. Substituting the Hamiltonian (3.1) in (2.16), we obtain

$$\left[\frac{d}{dt} + \gamma_{\mathbf{k}} + i \left(\tilde{\omega}_{\mathbf{k}} - \frac{\omega_p}{2} \right) \right] c_{\mathbf{k}} + i P_{\mathbf{k}} c_{\mathbf{k}}^* = 0. \quad (3.3)$$

These equations differ from the linear equations given by (2.19), which describe parametric instability, only by frequency renormalization $\omega_{\mathbf{k}} \rightarrow \tilde{\omega}_{\mathbf{k}}$ due to the first sum in (3.1),

$$\tilde{\omega}_{\mathbf{k}} = \omega_{\mathbf{k}} + 2 \sum_{\mathbf{k}'} T_{\mathbf{k}\mathbf{k}'} |c_{\mathbf{k}'}|^2 \quad (3.4)$$

and the renormalization of the pump (2.29), which is described by the second sum (3.1).

If we substitute $c_{\mathbf{k}} = |c_{\mathbf{k}}| e^{i\varphi_{\mathbf{k}}}$ in (3.1), and evaluate $\partial \varphi_{\mathbf{k}} / \partial t$, we obtain $\partial / \partial t (\varphi_{\mathbf{k}} + \varphi_{-\mathbf{k}}) = 0$ which demonstrates the neutral stability of the phase difference within the framework of the theory using the diagonalized Hamiltonian (3.1). This was, in fact, to be expected because the phase difference between progressive waves travelling in opposite directions defines the position in space of the nodes of the resulting standing wave which, in a uniform pump field, is not fixed in any way.

The neutral equilibrium of the phase differences ensures that they can be randomized by any small perturbation, for example, by small random inhomogeneities or shape imperfections in the crystal. The reason why the phases become random can be found in the "residual" interaction which was not taken into account in the diagonalized Hamiltonian (3.1). Moreover, this interaction leads to a certain correlation between the phase differences in different pairs, but this correlation and the nondiagonal terms in the Hamiltonian \mathcal{H}_{int} remains small. A detailed discussion of this question, and a justification of the approximation in (3.1), is given in [33]. It is shown in that paper that the approximation defined by (3.1) is satisfactory for external-field amplitudes up to $h^* \sim h_1 [(k \partial \omega / \partial k) / \gamma]^{1/2}$ where h_1 is the threshold amplitude of the external field. In the case of parallel pumping, this yields $h^* \sim 100h_1$ for YIG.

The theory based on the diagonalization of the Hamiltonian, so that it takes the form given by (3.1), will be referred to as the S theory. This designation reflects the determining influence of the coefficients $S_{\mathbf{k}\mathbf{k}'}$ on the nonlinear behavior of a set of parametric waves.

Henceforth we shall suppose that the individual wave media are random, and that averaging has been carried out over their ensemble. The turbulence is then described in the language of correlation functions

$$\langle a_{\mathbf{k}} a_{\mathbf{k}'}^* \rangle = n_{\mathbf{k}} \delta(\mathbf{k} - \mathbf{k}'), \quad \langle a_{\mathbf{k}} a_{\mathbf{k}'} \rangle = \sigma_{\mathbf{k}} \delta(\mathbf{k} + \mathbf{k}').$$

The quantities $n_{\mathbf{k}}$ and $\sigma_{\mathbf{k}}$ have the dimensions of action (erg.sec). The equations for these quantities can readily be obtained by direct averaging of (3.3):

$$\begin{aligned} \frac{1}{2} \frac{\partial n_{\mathbf{k}}}{\partial t} &= n_{\mathbf{k}} (-\gamma_{\mathbf{k}} + \text{Im } P_{\mathbf{k}}^* \sigma_{\mathbf{k}}), \\ \frac{1}{2} \frac{\partial \sigma_{\mathbf{k}}}{\partial t} &= \sigma_{\mathbf{k}} \left(i \tilde{\omega}_{\mathbf{k}} - \frac{i \omega_p}{2} - \gamma_{\mathbf{k}} \right) + \frac{i}{2} (n_{\mathbf{k}} + n_{-\mathbf{k}}) P_{\mathbf{k}}. \end{aligned} \quad (3.5)$$

It follows that

$$\begin{aligned} \left(\frac{\partial}{\partial t} + \gamma_{\mathbf{k}} \right) (n_{\mathbf{k}} n_{-\mathbf{k}} - |\sigma_{\mathbf{k}}|^2) &= 0, \\ \left(\frac{\partial}{\partial t} + 2\gamma_{\mathbf{k}} \right) (n_{\mathbf{k}} - n_{-\mathbf{k}}) &= 0, \end{aligned}$$

which show that arbitrary initial conditions relax in a time of the order of $1/\gamma$ to a state (not necessarily a stationary state) in which $n_{\mathbf{k}} = n_{-\mathbf{k}}$; $|\sigma_{\mathbf{k}}| = n_{\mathbf{k}}$.

The condition $|\sigma_{\mathbf{k}}| = n_{\mathbf{k}}$ means that the phases of wave pairs are fully correlated. In this case, we may write

$$\sigma_{\mathbf{k}} = n_{\mathbf{k}} e^{-i\psi_{\mathbf{k}}}.$$

In terms of these variables, we can write (3.5) and the definitions given by (3.4) and (2.29) in the form

$$\frac{dn_{\mathbf{k}}}{2dt} = n_{\mathbf{k}} \left[-\gamma_{\mathbf{k}} + \text{Im} (P_{\mathbf{k}}^* e^{-i\psi_{\mathbf{k}}}) \right], \quad (3.6)$$

$$\frac{d\psi_{\mathbf{k}}}{2dt} = \tilde{\omega}_{\mathbf{k}} - \frac{\omega_p}{2} + \text{Re} (P_{\mathbf{k}}^* e^{-i\psi_{\mathbf{k}}}), \quad (3.7)$$

$$\tilde{\omega}_{\mathbf{k}} = \omega_{\mathbf{k}} + 2 \sum_{\mathbf{k}'} T_{\mathbf{k}\mathbf{k}'} n_{\mathbf{k}'}, \quad (3.7)$$

$$P_{\mathbf{k}} = \hbar V_{\mathbf{k}} + \sum_{\mathbf{k}'} S_{\mathbf{k}\mathbf{k}'} n_{\mathbf{k}'} e^{-i\psi_{\mathbf{k}'}}. \quad (3.8)$$

It is useful to note that the variables $n_{\mathbf{k}}$ and $\psi_{\mathbf{k}}$ are canonical, with the Hamiltonian given by

$$\begin{aligned} \mathcal{H}_S = 2 \sum_{\mathbf{k}} n_{\mathbf{k}} \left\{ \left(\omega_{\mathbf{k}} + \sum_{\mathbf{k}'} T_{\mathbf{k}\mathbf{k}'} n_{\mathbf{k}'} - \frac{\omega_p}{2} \right) \right. \\ \left. + \left[\hbar V_{\mathbf{k}} \cos \psi_{\mathbf{k}} + \frac{1}{2} \sum_{\mathbf{k}'} S_{\mathbf{k}\mathbf{k}'} n_{\mathbf{k}'} \cos (\psi_{\mathbf{k}} - \psi_{\mathbf{k}'}) \right] \right\}. \end{aligned} \quad (3.9)$$

In fact, it is readily verified that (3.6) is obtained by varying \mathcal{H}_S according to the rule

$$\frac{dn_{\mathbf{k}}}{dt} + 2\gamma_{\mathbf{k}} n_{\mathbf{k}} = -\frac{\delta \mathcal{H}_S}{\delta \psi_{\mathbf{k}}}, \quad \frac{d\psi_{\mathbf{k}}}{dt} = \frac{\delta \mathcal{H}_S}{\delta n_{\mathbf{k}}}. \quad (3.10)$$

These equations show that (3.6) are Hamiltonian equations, so that the determination of the turbulence spectrum within the framework of the S-theory is a purely dynamic problem.

(b) Ground state. External stability condition. We must now consider the stationary states of a system of pairs in which all the amplitudes $n_{\mathbf{k}}$ and phases $\psi_{\mathbf{k}}$ are time-independent. Assuming that $n_{\mathbf{k}} = \psi_{\mathbf{k}} = 0$ in (3.6), we immediately obtain the following condition for all points in \mathbf{k} space for which $n_{\mathbf{k}} = 0$:

$$|P_{\mathbf{k}}|^2 = \gamma_{\mathbf{k}}^2 + \left(\tilde{\omega}_{\mathbf{k}} - \frac{\omega_p}{2} \right)^2. \quad (3.11)$$

Before we analyze this result, we must note two general points. Firstly, it is clear that the pair amplitudes are nonzero only in a thin layer near the resonance surface $2\tilde{\omega}_{\mathbf{k}} = \omega_p$. This means that it is convenient to use the following coordinates in \mathbf{k} space: κ the deviation from this surface in the normal direction, and Ω is the coordinate on the surface.

Secondly, the coefficients in (3.6) which have the

dimensions of frequency (γ_k , hV_k , $\Sigma T_{kk'} n_k$, $\Sigma S_{kk'} n_k e^{-i\psi_k}$) are much smaller than the natural frequency ω_k . It follows that it is sufficient to take a dependence on k only for $(\omega_k - 1/2\omega_p)$, and to replace all the remaining coefficients by their values on the resonance surface, i.e., γ_Ω , hV_Ω , $T_{\Omega\Omega'}$, and $S_{\Omega\Omega'}$, respectively.

If we use the above approximation, we can readily find from (3.11) those values of κ for which $n_{k\Omega} \neq 0$:

$$\tilde{\omega}_{k\Omega} = \frac{\omega_p}{2} \pm \sqrt{|P_\Omega|^2 - \gamma_\Omega^2}. \quad (3.12)$$

Therefore, in the stationary state, the pair-amplitude distribution is singular: $n_{k\Omega} \neq 0$ only on the two surfaces (3.12). However, there is an infinite set of such stationary states which differ both in the form of these surfaces and in the distribution of $n_{k\Omega}$ over them. In point of fact, the directions Ω in which $n_{k\Omega}$ is zero can be specified arbitrarily. In reality, of all the stationary states, only those can be realized that are stable against small perturbations. The requirement of stability imposes a strong restriction on the class of possible stationary states.

It is clear that the study of the stability of stationary states within the framework of the diagonalized Hamiltonian divides into two independent problems: the problem of the internal stability against perturbations in the amplitudes and phases of existing pairs, and external stability against the creation of new pairs.

External stability is the simplest to consider. Thus, we can use (3.3) to write down the equations for a pair of perturbation waves

$$c_q, c_{-q}^* \sim e^{v_q t}$$

outside the surfaces (3.12). Neglecting the dependence of P_k and γ_k on κ , we obtain the following expression for the growth rate:

$$v_q = -\gamma_\Omega + \sqrt{|P_\Omega|^2 - \left(\tilde{\omega}_q - \frac{\omega_p}{2}\right)^2},$$

which is analogous to (2.20). The growth rate v_Ω which is a maximum in $|q|$ (with fixed Ω) corresponds to $2\tilde{\omega}_q = \omega_p$, i.e., it lies halfway between the surfaces (3.12):

$$v_\Omega = -\gamma_\Omega + |P_\Omega|.$$

The external stability condition, $v_\Omega \leq 0$, can therefore be written in the form

$$|P_\Omega| \leq \gamma_\Omega.$$

On the other hand, it follows from (3.12) that $|P_\Omega| \geq \gamma_\Omega$ for those directions Ω in which $n_{k\Omega} \neq 0$. Consequently, for these directions, the two inequalities are consistent only when $|P_\Omega| = \gamma_\Omega$. The two surfaces (3.12) then merge into one:

$$2\tilde{\omega}_{k_0} = \omega_p. \quad (3.14)$$

Therefore, for a given distribution of wave amplitudes over the angles, the condition of external stability completely removes the ambiguity in the choice of the surface on which $n_k \neq 0$. This surface (3.14) will be called the "resonance surface," and the stationary state with external stability will be referred to as the "ground state."

The above result has a simple physical interpretation. It is clear from (2.20) and (2.21) that, during the linear stage, the waves which are most strongly coupled to the

pump are those for which the frequency detuning is $\tilde{\omega}_k - 1/2\omega_p = 0$. The difference $\tilde{\omega}_k - 1/2\omega_p$ is the frequency detuning with nonlinear terms included. When it is not equal to zero at points at which n_k is localized, then there is a region in k -space such that pairs contained by it are more strongly coupled to the pump than the existing pairs, and we have the possibility of parametric excitation of such pairs.

It is interesting to examine in detail how, during the development of parametric instability, the spin-wave state $n_k \sim \delta(k - k_0)$, which is coherent in the modulus of k , arises out of the thermal noise $n_k^0 = T/\omega_k$. We have investigated this problem^[24] both analytically and numerically on a computer. We found, in particular, that after a certain interval following the introduction of the pump, the distribution of waves over the modulus of k can be described by a gaussian, the width of which tends to zero as $(t)^{-1/2}$.

Our next problem is to investigate the distribution of pairs on the resonance surface (3.14). We shall introduce the distribution function N_Ω which gives the "number" of pairs per unit solid angle. This function is defined by

$$N = \sum_k n_k = \int N_\Omega d\Omega. \quad (3.15)$$

The stationary equations for N_Ω and ψ_Ω which follow from (3.6)–(3.8) and (3.14) can be written in the form

$$(P_\Omega e^{i\psi_\Omega} - i\gamma_\Omega) N_\Omega = 0, \quad P_\Omega = hV_\Omega + \int S_{\Omega\Omega'} N_{\Omega'} e^{-i\psi_{\Omega'}} d\Omega'. \quad (3.16)$$

These equations do not as yet define unambiguously the distribution of N_Ω and ψ_Ω because the surfaces on which $N_\Omega = 0$ can be chosen arbitrarily. The requirement of external stability will be shown in the next section to reduce substantially the class of possible solutions, and in a number of cases the stable distributions are unique.

The condition of external stability can usefully be interpreted in terms of the following geometric ideas. The expressions $\gamma = \gamma_\Omega$ and $P = P_\Omega$ are the equations of surfaces in k space. Condition (3.13) means that the surface P lies wholly inside the surface γ and touches it at points Ω at which the solution is concentrated. Since $V_k = V_{-k}$ and $S_{kk'} = S_{k-k'}$, both these surfaces have a center of symmetry. The γ and P surfaces can touch either at a discrete number of points, or over a continuum, i.e., a line or even a piece of the surface. In the former case we have a finite number of monochromatic pairs, and in the latter a continuous distribution of N_Ω . An intermediate situation is also possible in which the surfaces touch at an isolated pair of points and, in addition, along a certain line. The system then contains a monochromatic pair and a continuous background. We note that the question of the validity of the S theory in the presence of a small number of discrete pairs requires special consideration, including the examination of stability within the framework of the exact Hamiltonian (see below).

(c) Stage-by-stage excitation. We must now consider the distribution of parametrically excited waves over the resonance surface for different values of the external field h , beginning with the threshold value.

In studying the distribution N_Ω we shall largely confine our attention to the axially-symmetric case which is realized in isotropic and cubic ferromagnets mag-

netized along the $\langle 111 \rangle$ or $\langle 100 \rangle$ axis. The coupling coefficient is then given by (2.26), and the coefficients describing the interaction are given by

$$S_{\Omega\Omega'} = S(\theta, \theta'; \varphi - \varphi'), \quad T_{\Omega\Omega'} = T(\theta, \theta'; \varphi - \varphi'). \quad (3.17)$$

It is clear from the axial symmetry that, in the stationary state, the amplitude of the pairs $N_\Omega \equiv N_{\theta, \varphi}$ is independent of the azimuthal angle φ . We shall define the amplitude N_θ by

$$N_{\theta, \varphi} = 2\pi N_\theta,$$

so that

$$N = \int N_\Omega d\Omega = \int N_\theta \sin \theta d\theta.$$

From the equations for n_k it is also clear that the quantity $P_k^* \delta_k$ is also independent of φ . Since $V_k = V_\theta e^{2i\psi}$ [see (2.26)], we have

$$\psi_\Omega \equiv \psi_{\theta, \varphi} = \psi_\theta + 2\varphi. \quad (3.18)$$

These relationships enable us to eliminate the dependence on φ in (3.16), and write it in the form

$$(P_\theta e^{i\psi_\theta} - i\gamma_\theta) N_\theta = 0, \\ P_\theta = P_\Omega e^{-2i\varphi} = hV_\theta + \int S_{\theta\theta'} N_{\theta'} e^{-i\psi_{\theta'}} \sin \theta' d\theta', \quad (3.19)$$

where

$$S_{\theta\theta'} = \frac{1}{2\pi} \int_0^{2\pi} S(\theta, \theta'; \varphi - \varphi') e^{2i(\varphi - \varphi')} d(\varphi - \varphi'), \quad (3.20)$$

To determine the distribution N_θ for small excesses above the threshold, we shall use the above geometric interpretation of the external stability condition [given by (3.13)]. For very small excesses above the threshold, when the amplitudes N_θ are small, the surface $|P_\theta|$ is not very different from the hV_θ surface which has a maximum on the equator at $\theta = 1/2\pi$. The curvatures of these surfaces (second derivatives with respect to θ) are also very similar. Hence it is clear that the surfaces of $|P_\theta|$ and γ_θ touch one another only along the line $\theta = 1/2\pi$. This means that, for small excesses above the threshold, the distribution N_θ is nonzero only along this line:

$$N_\theta = N_1 \delta\left(\theta - \frac{\pi}{2}\right). \quad (3.21)$$

For the integral amplitude $N_1 = \sum_k |c_k|^2$ and phase $\psi_1 = \psi_1/2\pi$ we can readily show, using (3.19), that

$$N_1 = \frac{\sqrt{h^2 V_1^2 - \gamma_1^2}}{|S_{11}|}, \quad \sin \psi_1 = \frac{\gamma_1}{hV_1}. \quad (3.22)$$

where

$$V_1 = V_{\pi/2}, \quad S_{11} = S_{\pi/2, \pi/2}, \quad \gamma_1 = \gamma\pi/2.$$

The geometric ideas used above can readily be generalized to the case of an arbitrary dependence on V_Ω . It can be shown^[20] that, in general, and when the excess above the threshold is sufficiently small, N_Ω is different from zero only at those points on the resonance surface where $|V_\Omega|$ is a maximum. In the case of spherical symmetry, these are points of the entire surface, whereas for axial symmetry they are points on one ($\theta = 1/2\pi$) or two lines. In the case of lower symmetries, this is one or a few equivalent pairs of points. It is interesting that the integral amplitude is not very sensitive to the degree of symmetry of the problem. It is given by (3.22) in which $V_1 = \max |V_\Omega|$

and S_{11} is the mean value of $S_{\Omega\Omega'}$ on a set of points where $N_\Omega \neq 0$.

We shall show that the pair distribution function (3.21), which is localized on the equator, conserves stability against pair creation at other latitudes up to sufficiently large excesses above the threshold. To show this, consider the function $|P_\theta|$. From (3.19), (3.21), and (3.22) we have

$$|P_\theta|^2 = N_1^2 \left(S_{11} \frac{V_0}{V_1} - S_{\theta 1} \right)^2 + \frac{V_0^2}{V_1^2} \gamma_1^2.$$

It is clear that the state described by (3.21) will be stable for $|P_\theta|^2 < \gamma_\theta^2$ for all θ except for $\theta = 1/2\pi$. The "second threshold" $h = h_2$ corresponds to the minimum value of h for which the surfaces $|P_\theta|$ and γ_θ touch for some value $\theta = \theta_2$ not equal to $1/2\pi$. Therefore $h_2 = \min h_\theta$ for $\theta = \theta_2$ where h_θ is determined from the condition $|P_\theta| = \gamma_\theta$,

$$h_2^2 = h_1^2 \left[1 + \frac{S_{11}^2}{\gamma_1^2} \frac{V_0^2 V_1^2 - \gamma_1^2 V_0^2}{(S_{11} V_1 - S_{\theta 1} V_0)^2} \right]. \quad (3.23)$$

For the simple assumptions $\gamma_\theta = \gamma$ and $S_{\theta 1} = 0$ we find that $h_2^2/h_1^2 = 2$ for $\theta_2 = 0$. In reality, on the other hand, for cubic ferromagnets the function $S_{\theta 1}$ is very different from a constant, and this leads to a much higher second threshold.

Symmetry considerations show that $S_{\theta 1} = S(\sin^2 \theta)$, $S_{\theta 1}(0) = 0$, i.e.,

$$S_{\theta 1} = S_1 \sin^2 \theta + S_2 \sin^4 \theta + \dots \quad (3.24)$$

The expressions for the coefficients S_1, S_2 are in general highly unwieldy. As an example, consider the expression for $S_{\theta 1}$ in the case where the wave vector of the parametric waves tends to zero^[23].

$$S_{\theta 1} = 2\pi g^2 \left(\frac{\omega_M}{\omega_p} \right) \left\{ \sin^2 \theta \left[\frac{\omega_M}{\omega_p} (N_z - 1) \right. \right. \\ \left. \left. + \frac{1}{2} \sqrt{1 + \left(\frac{\omega_M}{\omega_p} \right)^2} + \frac{1}{2} \sqrt{1 + \left(\frac{\omega_M}{\omega_p} \right)^2 \sin^4 \theta} \right] \right. \\ \left. + \sin^2 2\theta \frac{\omega_M}{\omega_p} \left[\sqrt{1 + \left(\frac{\omega_M}{\omega_p} \right)^2 \sin^4 \theta} - \frac{\omega_M}{\omega_p} \sin^2 \theta \right] \right\}. \quad (3.25)$$

To estimate the height of the second threshold, we shall restrict our attention to the two terms in the expansion in (3.24) and substitute $\gamma_0 = \text{const}$. In that case

$$\left(\frac{h_2}{h_1} \right)^2 = 1 + 11 \left(\frac{S_1 + S_2}{S_2} \right)^2 \theta_2 \approx 50^\circ. \quad (3.26)$$

From (3.25) we have for $\omega_M \ll \omega_p$

$$S_1 + S_2 \approx 2\pi g^2 \left(\frac{\omega_M}{\omega_p} \right)^2 \left[N_z - 1 + \sqrt{1 + \left(\frac{\omega_p}{\omega_M} \right)^2} \right], \\ S_2 \approx 2\pi g^2 \left(\frac{\omega_M}{\omega_p} \right)^2 \left(4 - 2 \frac{\omega_M}{\omega_p} \right).$$

For example, for a YIG sphere with $\omega_p/\omega_M = 1.9$ we have $(h_2/h_1)^2 \approx 3.5$ (for 5.5 dB). The presence of only one group of waves for $h_1 < h < h_2$ on the equator of the resonance surface, and the threshold excitation of the second group well away from the equator for $h = h_2$ enables us to speak of a stage-by-stage excitation of waves during parametric instability. The step-by-step excitation of spectra which are singular in k space is a characteristic feature of S theory. This type of excitation of waves can be compared with the description of the origin of turbulence for small Reynolds numbers given by Landau^[44]. The successive switching on of new groups of waves with increasing departure from the threshold is basically the same as the idea^[41] of an increasing number of degrees of freedom as one approaches developed turbulence.



FIG. 4. Emission into the 'perpendicular' channel as function of pump power (YIG sphere, $M \parallel \langle 100 \rangle$).

A direct experiment designed to establish the presence of the second threshold is described in^[21]. It can be summarized as follows. The YIG specimen was placed in a resonator with two degenerate orthogonal modes, the magnetic field of which, h and h_{\perp} , was respectively parallel and perpendicular to the magnetization M . The parallel channel was used for the parametric excitation of spin waves and the orthogonal channel for the detection of the emission from the specimen at the pump frequency. A sharp increase in the radiated power into the perpendicular channel at about 8–12 dB above the threshold was observed (Fig. 4), depending on the constant magnetic field, and the orientation and shape of the specimen.

The resonator mode with polarization $h \perp M$ was excited by the homogeneous precession of magnetization which in turn is "unwound" by the parametric spin waves. This process is described by the Hamiltonian

$$\mathcal{H} = \frac{1}{2} \sum_k (u_k^* b_k b_{-k} + \text{c. c.}),$$

in which $u_k = u \sin 2\theta e^{i\varphi}$. Hence the power radiated into the transverse channel is given by

$$P_{\perp} \sim |\sum_k u_k b_k b_{-k}|^2,$$

which vanishes when $\theta = 0$ and $\theta = 1/2\pi$. The function $P_{\perp}(h)$ in Fig. 4 thus clearly shows that the only pairs excited in the interval 0–9 dB are those with $\theta = 1/2\pi$. The power P_{\perp} emitted for large excesses above the threshold is naturally associated with the excitation of the second group of pairs with $\theta = 1/2\pi$.

The second threshold can also be determined from certain indirect observations, for example, the characteristic distortion of the top of the pump pulse, or the break on the curve showing the real susceptibility χ' as a function of the pump power (see next section). The series of thresholds discovered by Petrakovskii and Berzhanskii, who used the distortion of the pump pulse,^[45] appears to have been connected with the step-by-step excitation of parametric spin waves.

In conclusion, we must describe, at least qualitatively, the behavior of parametric spin waves for $h > h_2$. We can readily verify that the state with two groups of pairs at latitudes θ_1 and θ_2 becomes unstable for a particular departure from the threshold h_3 , and a third group is created at the latitude θ_3 . The next group appears at h_4 , and so on. The question as to what happens when h is increased still further is discussed in^[20]. For large h/h_1 the distribution of N_{Ω} is very sensitive to the fine structure of the quantities V_{Ω} and $S_{\Omega\Omega'}$. In some cases, a continuous distribution of pairs over the resonance surface is established, whilst in other cases the limitation mechanism cuts off and an essentially nonsta-

tionary situation appears. The nondiagonal terms in the Hamiltonian, which smooth out distributions which are singular in the angles, begin to play an appreciable role as the number of discrete groups of pairs increases.

(d) Nonlinear susceptibilities. In Sec. 2 we noted that the main experimental characteristics of a system of parametric waves are the nonlinear susceptibilities χ' and χ'' which are given by (2.33) and (2.34). In the case of axial symmetry, we have from (3.18) and (3.19)

$$\begin{aligned} \chi'' &= \frac{2 \sum_{\theta} V_{\theta} N_{\theta} \sin \psi_{\theta}}{h} = \frac{2 \sum_{\theta} \gamma_{\theta} N_{\theta}}{h^2}, \\ \chi' &= \frac{2 \sum_{\theta} V_{\theta} N_{\theta} \cos \psi_{\theta}}{h} = \frac{2 \sum_{\theta\theta'} S_{\theta\theta'} N_{\theta} N_{\theta'} \cos(\psi_{\theta} - \psi_{\theta'})}{h^2}. \end{aligned} \quad (3.27)$$

It is clear from these formulas that the imaginary susceptibility χ'' characterizes only the integral pair intensity, whereas the real susceptibility χ' is also a function of the phase relationships between the pairs. The quantity χ' is thus a better characteristic of the system because it is sensitive to the details of the pair distribution in space, auto-oscillations, inhomogeneities, and so on. This is the reason for the considerable spread in the experimental values of χ' reported by different workers. Thus, for example, in one of the first papers^[25] it was reported that $\chi'/\chi'' \approx 0.1$ for YIG, and that this ratio is not very dependent on the magnetic field. The low value of this ratio was used as a basis for the suggestion that the limiting mechanism is some kind of nonlinear damping leading to $\chi' \approx 0$ ^[35, 36]. The behavior of the spin waves beyond the parametric excitation threshold is described in^[37]. In particular, this monograph describes the "self-suppression" mechanism for the amplitude, but again assumes that $\chi'/\chi'' \ll 1$.

Subsequent careful studies of χ' and χ'' showed, however, that in perfect single crystals, and in the absence of auto-oscillations, the quantity χ' is not small and may even exceed χ'' ^[23, 46].

Figure 5 shows the characteristic functions $\chi'(h^2)$ and $\chi''(h^2)$ for a YIG sphere along the three principal

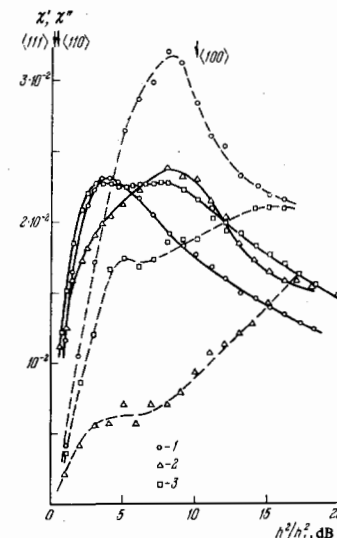


FIG. 5. Measured real χ' (dashed line) and imaginary χ'' (solid line) components of longitudinal susceptibility as functions of pump power for YIG sphere. 1— $\langle 100 \rangle$ orientation, 2— $\langle 111 \rangle$ orientation, 3— $\langle 110 \rangle$ orientation. Arrows indicate excitation thresholds for the auto-oscillations.

crystallographic directions: along the $\langle 100 \rangle$ direction when there are no auto-oscillations in magnetization, and along the $\langle 111 \rangle$ and $\langle 110 \rangle$ directions when there are strong auto-oscillations. It is clear that the auto-oscillations in magnetization have no substantial influence on χ'' , but may reduce χ' by a substantial factor.¹⁾ This fact can be explained as follows. When the excess above the instability threshold is large

$$\sin \psi \approx h_1/h \ll 1,$$

$$|\cos \psi| \approx 1 - \frac{1}{2} \left(\frac{h_1}{h} \right)^2,$$

i.e., the cosine of the phase shift for the pairs relative to the pump, which determines χ' , is near its extremal value. The development of auto-modulation which leads to a periodic variation in the angle ψ does not affect the average of $\sin \psi$ but reduces the mean value of $\cos \psi$ and at the same time the magnitude of the susceptibility χ' .

The fact that $\chi'/\chi'' \approx 1$ is an unambiguous indication of an important phase mismatch between the pump and the spin-wave pairs, which follows from the S-theory. Comparison with the experimental dependence of χ' and χ'' on h is greatly facilitated when the excess above the threshold is small ($h \lesssim 2h_1$) and only the equatorial pairs with $\theta = 1/2\pi$ are excited. In this case, we have from (3.27) and (3.22)

$$\chi'' = \frac{2V_1^2 h_1}{S_{11}} \frac{\sqrt{h_2 - h_1^2}}{h^2}, \quad \chi' = \frac{2V_1^2}{S_{11}} \frac{h^2 - h_1^2}{h^2}. \quad (3.28)$$

Graphs of these functions are shown in Fig. 2. It is clear that there is a similarity between the theoretical and experimental curves. For example, in accordance with the theory, the curve showing χ' cuts the χ'' curve at the maximum. The discrepancy between the theoretical and experimental curves representing $\chi'(h^2)$ for $h^2 > 8$ dB is naturally explained by the excitation of the second group of pairs which are not taken into account in (3.28).

Numerical calculations were carried out on a computer in order to compare the S-theory with experiments for large excesses above the threshold^[23]. The first step was to compute the coefficients $S_{\theta\theta'}$ for particular experimental situations involving YIG. In this calculation, use was made of only the known values of the main YIG parameters, i.e., magnetization, crystallographic anisotropy field, and exchange field. The values of $S_{\theta\theta'}$ obtained in this way were substituted into the nonstationary equation of motion (3.3), which was then solved on the computer by time iteration from the thermal noise level. The computed stationary values of the amplitude and phase for different excesses above the threshold were then used to determine χ' and χ'' from (3.27). The results of these calculations are shown in Fig. 6 together with the laboratory data. It is clear there is not only a qualitative but also good quantitative agreement between theory and experiment.

Table I compares theoretical and experimental values of the maximum susceptibility $\chi_m'' = \max \chi''(h)$ for different cubic ferromagnets of spherical shape. We have measured the susceptibility of YIG by the standard methods described in Sec. 2. The quantity χ_m'' for other crystals was measured with the same apparatus through a comparison with YIG. Theoretical values of χ_m'' were calculated from (3.28):

$$\chi_m'' = \frac{V_1^2}{S_{11}}, \quad (3.29)$$

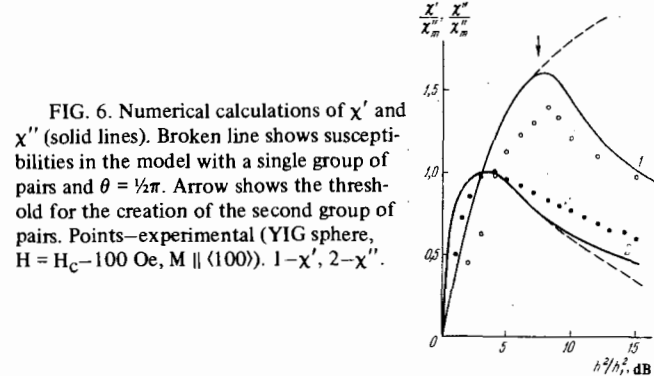


FIG. 6. Numerical calculations of χ' and χ'' (solid lines). Broken line shows susceptibilities in the model with a single group of pairs and $\theta = 1/2\pi$. Arrow shows the threshold for the creation of the second group of pairs. Points—experimental (YIG sphere, $H = H_c - 100$ Oe, $M \parallel \langle 100 \rangle$). 1— χ' , 2— χ'' .

TABLE I

Crystal	$\frac{4\pi M}{G}$	$H_A = \frac{\omega_a}{g}$	$2\Delta H_k = \frac{\gamma}{g}$	$\chi_m'' \cdot 10^3$		Orientation
				Experiment	Theory	
1. $Y_3Fe_5O_{12}$ (YIG)	1750	84	0.12	24 ± 5	21	(100)
2. $Y_3Fe_{4.3}Se_{0.6}O_{12}$	1500	8	0.36	23	22	(100)
3. $Bi_{0.2}Ca_{0.8}Fe_{3.6}V_{1.4}O_{12}$	650	58	0.45	5	7.5	(100)
4. $Li_{0.5}Fe_{2.5}O_4$	3700	580	0.80	80	70	(111)
5. $NiFe_2O_4$	3200	490	1.40	25	19	(100)
				55	84	(111)

which for cubic ferromagnets with axial symmetry ($M \parallel \langle 111 \rangle, \langle 100 \rangle$) assumes the form^[23]

$$\chi_m'' = \frac{1}{8\pi} \left| \frac{1}{N_z - 1 + \beta(\omega_a/\omega_M) + \sqrt{(\omega_p/\omega_M)^2 + 1}} \right|, \quad (3.30)$$

where we have substituted the expression V_1 and S_{11} , and

$$\beta = \begin{cases} -8 & \text{for } M \parallel \langle 111 \rangle, \\ +9 & \text{for } M \parallel \langle 100 \rangle. \end{cases}$$

It is clear from Table I that the simple formula given by (3.30) provides a good description of the absolute post-threshold susceptibility for a broad class of cubic ferromagnets. The discrepancy between theory and experiment in the case of $NiFe_2O_4$ (the $\langle 111 \rangle$ orientation) is probably connected with the fact that, in this case, the susceptibility maximum lies beyond the threshold for the second group of pairs, when (3.30) is no longer valid.

The susceptibility χ_m'' was measured in^[47] for the uniaxial ferromagnet $Ba_2Zn_2Fe_{12}O_{14}$ with "easy plane" anisotropy, and the anomalously large result $\chi_m'' = 0.2$ was obtained. Theoretical estimates of this parameter based on (3.29) using V_1 and S_{11} without taking into account the dipole-dipole interaction (for $\omega_M < \omega_a$, $\omega_p \lesssim \omega_a$) yields

$$\chi_m'' = \frac{1}{2\pi} \frac{\omega_M \omega_a}{\omega_p^2}. \quad (3.31)$$

If, following^[47], we assume for $Ba_2Zn_2Fe_{12}O_{14}$ that $4M = 2850$ G, $\omega_a/g = 9900$ Oe, and suppose that the pump frequency is $\omega_p/g = 6300$ Oe, we obtain $\chi_m'' = 0.1$, which is in qualitative agreement with experiment.

The sign of the real susceptibility χ' is also of major interest. According to (3.28), the sign of χ' is the same as the sign of S_{11} , and for cubic ferromagnets is determined by the sign of the denominator in (3.30). In agreement with experiment, theory predicts that for weakly anisotropic crystals (Nos. 1, 2, and 3 in Table I) $\chi' > 0$; for crystals with considerable anisotropy (Nos. 4 and 5) $\chi' > 0$ for the $\langle 100 \rangle$ orientation and $\chi' < 0$ for the $\langle 111 \rangle$ orientation.

(e) Effect of nonlinear damping. We must now consider the role of nonlinear damping of spin waves in the limitation of their parametric instability. In a perfect crystal, the damping of parametric waves appears as a result of the interaction with the thermal spin-wave reservoir, and is due to coalescence processes between the parametric wave and the thermal wave

$$\omega_{\mathbf{k}_0} + \omega_{\mathbf{k}_1} = \omega_{\mathbf{k}_2}, \quad \mathbf{k}_0 + \mathbf{k}_1 = \mathbf{k}_2, \quad (3.32)$$

or the decay of the parametric wave into two thermal waves:

$$\omega_{\mathbf{k}_0} = \omega_{\mathbf{k}_1} + \omega_{\mathbf{k}_2}, \quad \mathbf{k}_0 = \mathbf{k}_1 + \mathbf{k}_2 \quad (3.33)$$

where $\omega_{\mathbf{k}_0}$ refers to the parametric wave, and $\omega_{\mathbf{k}_1}$ and $\omega_{\mathbf{k}_2}$ to thermal waves. Decay processes are allowed only for sufficiently short spin waves $k > k_s$. The quantity k_s can be calculated by analyzing the dispersion relation (2.6). For YIG it turns out that $k_s \sim 10^5 \text{ cm}^{-1}$. The damping rates due to these processes can be calculated from the kinetic equation for the thermal wave (see, for example, [31]). These rates are given by

$$\gamma_{\mathbf{k}_0} = 4\pi \int |V_{012}|^2 (n_{\mathbf{k}_1} - n_{\mathbf{k}_2}) \delta(\mathbf{k}_0 + \mathbf{k}_1 - \mathbf{k}_2) \delta(\omega_{\mathbf{k}_0} - \omega_{\mathbf{k}_1} - \omega_{\mathbf{k}_2}) d\mathbf{k}_1 d\mathbf{k}_2 \quad (3.34)$$

in the case of coalescence, and by

$$\gamma_{\mathbf{k}_0} = 2\pi \int |V_{012}|^2 (n_{\mathbf{k}_1} + n_{\mathbf{k}_2} + 1) \delta(\mathbf{k}_0 - \mathbf{k}_1 - \mathbf{k}_2) \delta(\omega_{\mathbf{k}_0} - \omega_{\mathbf{k}_1} - \omega_{\mathbf{k}_2}) d\mathbf{k}_1 d\mathbf{k}_2 \quad (3.35)$$

in the case of decay.

To calculate the linear damping, it is sufficient to substitute the thermodynamic equilibrium spectrum for $n_{\mathbf{k}}$ in (3.34) and (3.35). The presence of parametric waves leads to a dependence of $n_{\mathbf{k}}$ on their intensity. This effect was discussed qualitatively by Schlömann, [35] by Le Gall et al., [28] and by others. It was considered quantitatively in [48] and is the reason for the nonlinear damping of spin waves. When the magnitude of this effect is calculated, it is essential to take into account the fact that only a small fraction of the thermal waves interacts with the parametric waves. Their number is determined by the conservation laws (3.32) and (3.33). The change in $n_{\mathbf{k}}$ in this region may not therefore be small.

The character of the nonlinear damping depends on which of the three-wave relaxation mechanisms predominates. An unexpected result is that, in the decay part of the spectrum, where $\gamma_{\mathbf{k}_0}$ is determined by coalescence processes, the differential nonlinear damping turns out to be negative: $\partial\gamma/\partial N < 0$ (N is the number of parametric waves). In fact, in each coalescence event defined by (3.32), there is an increase in the number N_2 of magnons in the region \mathbf{k}_2 , and a reduction in the number N_1 of magnons in the region \mathbf{k}_1 . As a result, the difference $n_{\mathbf{k}_1} - n_{\mathbf{k}_2}$ and also the damping rate $\gamma_{\mathbf{k}_0}$ given by (3.34) are reduced. On the other hand, relaxation processes in a system of thermal magnons tend to return this difference to the thermodynamic equilibrium value. The competition between these processes determines the steady state value of $\gamma_{\mathbf{k}_0}$. To estimate it, let us write the balance equations in the form

$$\begin{aligned} \frac{dN}{2dt} &= -\gamma N + \text{pump}, \\ \frac{dN_1}{2dt} &= -\gamma_1(N_1 - N_1^0) - \gamma N, \\ \frac{dN_2}{2dt} &= -\gamma_2(N_2 - N_2^0) + \gamma N, \end{aligned}$$

where N_1^0 and N_2^0 are the thermodynamic equilibrium

values of N_1 and N_2 . In the stationary state, $\dot{N}_1 = \dot{N}_2 = 0$ and

$$N_1 - N_2 = N_1^0 - N_2^0 - \gamma N \left(\frac{1}{\gamma_1} + \frac{1}{\gamma_2} \right). \quad (3.36)$$

According to (3.34), the damping of parametric waves is given by $\gamma = c(N_1 - N_2)$. Substituting (3.36) into this expression, we obtain

$$\gamma = \gamma_0 \frac{1}{1 + cN(\gamma_1^{-1} + \gamma_2^{-1})}. \quad (3.37)$$

When the amplitude of the parametric waves is small ($cN < \gamma_1, \gamma_2$), this expression assumes the simpler form

$$\gamma \approx \gamma_0 - \eta_1 N, \quad \eta_1 = \gamma_0 c \left(\frac{1}{\gamma_1} + \frac{1}{\gamma_2} \right). \quad (3.38)$$

It can be shown [48] that the following order-of-magnitude result is valid: $c \approx |V|^2/\omega_{\mathbf{k}}$. This is in agreement with the estimate of the coefficients in the Hamiltonian for the four-wave interaction, S and T.

The fact that the differential nonlinear damping is negative means that it does not reduce, but on the contrary, increases the amplitude of the parametrically excited waves. Thus, when $k_0 < k_s$, the limitation of the parametric instability occurs only as a result of the phase mechanism.

It follows from (3.38) that the coefficient of negative nonlinear damping η_1 is proportional to the ratio of the damping of parametric and thermal waves, $\gamma_0/\gamma_{1,2}$. Analysis of (3.32) shows that when $k_0 \rightarrow 0$, we have $k_1, k_2 \rightarrow \infty$ and, as the damping of spin waves increases with increasing k , the influence of the negative nonlinear damping is unimportant when $k \ll k_s$, whereas for $k_0 \sim k_s$ it is comparable in order of magnitude with the effects of phase interactions. When $k > k_s$, the decay of parametric waves comes into play, and we can readily show that it leads to positive nonlinear damping. The sign of the nonlinear damping is determined by the competition between coalescence and decay. It is shown in [48] that when $k \gtrsim k_s$ the resulting nonlinear damping is positive

$$\gamma \approx \gamma_0 + \eta_2 N, \quad \eta_2 \sim \frac{|V|^2}{\omega_{\mathbf{k}}} \sim S,$$

and provides a contribution to the amplitude limitation, which is comparable with the contribution of the phase mechanism.

There is one further nonlinear damping mechanism, namely, the coalescence of two or more parametrically excited spin waves. This was put forward by Suhl and Gottlieb [36]. It leads to positive differential nonlinear damping. In the simple case of coalescence of two waves

$$\gamma_{\mathbf{k}_0} = \gamma_0 + \int \eta_{\mathbf{k}_0} \mathbf{k}'_0 n_{\mathbf{k}'_0} d\mathbf{k}'_0 \approx \gamma_0 + \eta_3 N, \quad N \approx \frac{|V|^2}{\omega_{\mathbf{k}}} \approx S.$$

In general, this process may compete with the phase mechanism. It is allowed for wave vectors $\mathbf{k}_0, \mathbf{k}'_0$ which are greater than some characteristic value k_{3M} . For example, if \mathbf{k}_0 and \mathbf{k}'_0 lie in the plane of the equator, then

$$6\omega_{ex}(k_{3M}l)^2 = \sqrt{\omega_p^2 + \omega_M^2}.$$

We note, however, that for cubic ferromagnets the coalescence of parametric waves is unimportant up to the threshold h_2 for the creation of the second group of pairs for any \mathbf{k} . This is explained by the fact that the first group of waves is excited exactly on the equator of the resonance surface ($\theta = 1/2\pi$), and the coefficient $\eta_{\mathbf{k}_0 \mathbf{k}'_0}$ is then identically zero (see [31]).

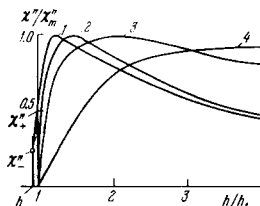


FIG. 7. Imaginary susceptibility χ'' as function of pump amplitude, with allowance for nonlinear damping, $\eta/|S| = -0.25$ (nonlinear damping), $\eta/|S| = 0$, $\eta/|S| = 0.25$, and $\eta/|S| = 1$ (curves 1–4 respectively).

Nonlinear damping can readily be introduced into the S theory calculations. All that is required is to replace γ by $\gamma + \eta N$. Figure 7 shows a graph of the function $\chi''(h^2)$ for different magnitudes and signs of the parameter η/S . Let us consider some of the characteristic features of these curves.

When $\eta > 0$, the $\chi''(h^2)$ curve has a finite slope at the threshold point, which is equal to V_1^2/η , and the final value is given by $\chi''(\infty) = \eta V_1^2/\eta^2 + S_{11}^2$. It is interesting that when $\eta < |S_{11}|$ the maximum value of χ'' is dependent on η and is given by (3.29). The nonlinear damping affects only the position h_m of the maximum, which shifts toward greater h as η increases: $h_m = \sqrt{2}h_1|S_{11}|/|S_{11}| - \eta$. When $\eta > |S_{11}|$ the susceptibility χ'' increases monotonically with increasing h .

It is interesting to note that, even when $|\eta| \ll |S|$, $\eta > 0$, the susceptibility χ' decreases rapidly (as compared with the case $\eta = 0$) in a narrow region near the threshold, and the $\chi'(h)$ curve has a zero tangent at $h = h_1$:

$$\chi' = \frac{2SV^2}{\eta^2} \left(\frac{h-h_1}{h_1} \right)^2$$

when

$$(hV - \gamma) \lesssim 2\eta V^2/S^2.$$

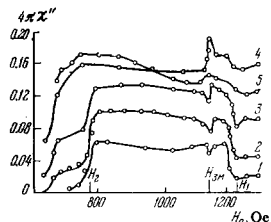
It may be that this is the reason why nonzero values of χ' were not established in [48] for YIG for excesses above the threshold less than $\sim 1-2$ dB.

For $\eta > 0$ hard excitation of parametric waves takes place and is accompanied by a hysteresis of the function $\chi''(h^2)$. When $|\eta| \ll S_{11}$ the reverse jump χ'' amounts to half the direct jump $\chi_+ - \chi_- = 1/2 \chi'' = 2|\eta|S_{11}/|S_m|^2$. It occurs for the pump amplitude $h_- = h_1|S_{11}|/(S_{11}^2 + \eta^2)^{1/2}$.

The phenomenon of hard excitation and the hysteresis of χ'' were discovered by Le Gall et al. [28] in single crystals of YIG at $\omega_p = 9.8$ GHz. The phenomenon was observed for fields in the range $H_2 < H < H_1$; the decay processes were "released" at H_2 and positive nonlinear damping was switched on, and for sufficiently large H_1 the effect vanished because the negative nonlinear damping was small.

Negative nonlinear damping will also lead to a characteristic dependence of χ'' on the constant magnetic field as shown in Fig. 8 [38]. As can be seen, the value of χ'' increases sharply at $H = H_1$ and $H = H_2$. The function $\chi''(H)$ exhibits an anomaly near $H = H_{3M}$ at which the coalescence of two parametric waves ($k = k_{S_1}$) comes into play. Near $H = H_{3M}$ there is a narrow resonance minimum which goes over into a resonance maximum as the excess above the threshold increases. This is in conflict with the original theory of Sühl and Gottlieb which predicted a sharp reduction in the susceptibility for fields $H < H_{3M}$ due to the introduction of the three-magnon coalescence mechanism. It is clear from Fig. 8 that a small jump (10%) is observed only for large excesses above the threshold. These facts are readily

FIG. 8. Measured χ'' as a function of the external magnetic field (YIG sphere, $M \parallel \langle 100 \rangle$). Curves 1–5 correspond to 0.5, 1, 2, 5, and 10 dB above the threshold.



understood within the framework of the foregoing discussion. Thus, for small excesses above the threshold, only waves with $\theta = 1/2\pi$ are excited and for these waves the coefficient V in (3.34), which describes the coalescence process, is equal to zero, as already noted. The slight spread of the distribution function N_0 , which is due to inhomogeneities and other factors, leads to a finite but small value of η_3 . The sharp increase in η_3 occurs only when the field reaches the value H_{3M} where, as can be readily verified, the integral in (3.40) has a resonance peak which is connected with the singularity of the density of states for which the coalescence process is allowed. The change in the sign of the resonance peak is explained by the fact that, for small excesses above the threshold, positive nonlinear damping reduces the magnitude of χ'' , and for large excesses it increases it (Fig. 7). It is also clear that the appearance of a jump in χ'' when the excess is greater than 8 dB is connected with the creation of a group of pairs with $\theta \neq 1/2\pi$.

4. COLLECTIVE EXCITATIONS AND AUTO-OSCILLATIONS OF MAGNETIZATION.

(a) The spectrum of collective oscillations. So far, we have confined our attention to stationary states of a system of parametric waves. In this section, we shall consider the behavior of the system as it departs from the stationary state. For the sake of simplicity, we shall initially neglect dissipation. The Hamiltonian of the system, \mathcal{H} , is then a constant of motion. Suppose that the perturbed-state Hamiltonian \mathcal{H} differs from the Hamiltonian \mathcal{H}_0 in the ground state. This means that the system can never reach the ground state, and since it has no other stable stationary states, its behavior will be essentially nonstationary. Two types of behavior are then possible: the system either executes small oscillations about the ground state, or departs completely from it. We shall show that both types of behavior are possible in the case of parametric excitation of spin waves.

Since we shall eventually have to compare theory with experiment, let us begin by considering the cubic ferromagnet magnetized along the $\langle 111 \rangle$ or $\langle 100 \rangle$ axes. For excesses above the threshold which lie below the second threshold, the spin waves are excited in the plane of the equator in the ground state.

Let α_k be the deviation of the complex amplitudes c_k from the ground state (3.21), (3.22), and let us isolate in the S-theory Hamiltonian (3.9) the part $\mathcal{H}^{(0)}$ which corresponds to the ground state, and the parts $\mathcal{H}^{(1)}$ and $\mathcal{H}^{(2)}$ which contain the linear and quadratic terms in α . Using the equations of motion, we can readily verify that the ground state is an extremum:

$$\mathcal{H}^{(1)} = 0.$$

The part of the Hamiltonian which is quadratic in small perturbations, assumes the form

$$\mathcal{H}^{(2)} = \frac{N_1}{(2\pi)^2} \left\{ 2 \int [S_{\varphi\varphi'} e^{i(\varphi-\varphi')} + T_{\varphi\varphi'} e^{i(\varphi'-\varphi)}] \alpha_\varphi \alpha_{\varphi'}^* d\varphi d\varphi' \right\}$$

$$+ \left[e^{i\Phi_1} \int T_{\varphi\varphi'} e^{-i(\varphi+\varphi')} \alpha_\varphi \alpha_{\varphi'} d\varphi d\varphi' + \text{c.c.} \right] \}, \quad (4.1)$$

where we have replaced summation by integration and $T_{\varphi\varphi'} = T_{\mathbf{k}\mathbf{k}'}, S_{\varphi\varphi'} = S_{\mathbf{k}\mathbf{k}'}$, for $\theta = \theta' = 1/2\pi, |\mathbf{k}| = |\mathbf{k}'| = k_0$. Transforming to the Fourier components

$$\alpha_m = \frac{1}{2\pi} \int_0^{2\pi} \alpha_\varphi e^{im\varphi} d\varphi$$

and using the axial symmetry of the situation

$$T_{\varphi\varphi'} = T(\varphi - \varphi'), \quad S_{\varphi\varphi'} = S(\varphi - \varphi'),$$

we obtain

$$\mathcal{H}^{(2)} = N_1 \sum_{m=-\infty}^{\infty} [2(T_m + S_m) \alpha_m \alpha_m^* + (T_m \alpha_m \alpha_{-m} + \text{c.c.})], \quad (4.2)$$

where²⁾

$$\begin{aligned} T_m &= \frac{1}{2\pi} \int_0^{2\pi} T(\varphi) e^{-im\varphi} d\varphi, \\ S_m &= \frac{1}{2\pi} \int_0^{2\pi} S(\varphi) e^{-i(m-2)\varphi} d\varphi. \end{aligned} \quad (4.3)$$

The Hamiltonian (4.2) can be diagonalized with the aid of the linear canonical transformation. Diagonalization is possible if

$$\frac{\Omega_m^2}{4N_1^2} = (T_m + S_m)^2 - T_m^2 = S_m(2T_m + S_m) > 0.$$

In this case, the Hamiltonian $\mathcal{H}^{(2)}$ can be written in the form

$$\mathcal{H}^{(2)} = \sum \Omega_m \beta_m \beta_m^*. \quad (4.4)$$

It is clear from (4.4) that the quantity

$$\Omega_m = \pm 2N_1 \sqrt{S_m(2T_m + S_m)}$$

is the frequency of collective oscillations in a system of spin waves. When $S_m(2T_m + S_m) < 0$, this frequency is imaginary. This indicates that the ground state is unstable against the excitation of exponentially growing oscillations (internal instability, see Sec. 3).

The canonical transformation uniquely determines the sign of the frequency Ω_m of collective oscillations. This sign can be determined from simple considerations. When $|T_m| \ll |T_m + S_m|$, the canonical transformation is such that the sign of Ω_m is the same as the sign of $S_m + T_m$. As T_m increases continuously, the sign of Ω_m remains the same. It changes only after Ω_m passes through zero. We then have $|T_m| = |T_m + S_m|$, and further increase in T_m is accompanied by the onset of instability. Thus, the signs of Ω_m and $T_m + S_m$ are always the same.

The fact that Ω_m is negative means that the energy of the spin-wave system decreases as a result of the excitation of collective oscillations. The energy of the system increases in the course of their relaxation. This is not inconsistent with the conservation of energy because the system of parametrically excited waves receives its energy from the pump.

The quantities S_m and T_m can be calculated for a cubic ferromagnet in the symmetric directions $\langle 111 \rangle$ and $\langle 100 \rangle$. It turns out that they differ from zero only when $m = 0, \pm 2$. The coefficients S_m and T_m corresponding to these modes are^[28]

$$S_0 = 2\pi g^2 \left(\frac{\omega_M}{\omega_p} \right)^2 \left[\sqrt{\frac{\omega_p^2}{\omega_M^2} + 1} + \tilde{N}_{z_0} - 1 \right], \quad (4.5)$$

$$T_0 = S_0 + 2\pi g^2 (\tilde{N}_{z_0} - 1), \quad (4.6)$$

$$\tilde{N}_{z_0} = N_z + \alpha \frac{\omega_a^2}{\omega_M^2}, \quad \beta = \begin{cases} -8 & \text{for } M \parallel \langle 111 \rangle, \\ +9 & \text{for } M \parallel \langle 100 \rangle, \end{cases} \quad (4.7)$$

$$T_{\pm 2} = 2\pi g^2 \left(\frac{\omega_M}{2\omega_p} \right)^2 \left[\tilde{N}_{z_0} - 1 + \sqrt{\left(\frac{\omega_p}{\omega_M} \right)^2 + 1} \right], \quad (4.8)$$

$$S_{\pm 2} = 2\pi g^2 \left[(\tilde{N}_{z_0} - 1) u_{\pm}^2 + \frac{\omega_M}{2\omega_p} u_{\pm} \right], \quad (4.9)$$

where

$$u_{\pm} = \frac{1}{2} \left(\sqrt{1 + \frac{\omega_M^2}{\omega_p^2}} \mp 1 \right), \quad \tilde{N}_{z_0} = \omega_{ex}(ak)^2 + \beta \frac{\omega_a}{\omega_M}.$$

These formulas show the dependence of the frequency of collective oscillations on the experimental conditions, namely, the excess above the threshold, pump frequency, magnetization, external magnetic field, shape of the specimen, and crystallographic anisotropy.

We must now consider the effect of the damping of spin waves on collective oscillations, especially since the damping γ_k may be of the same order as the frequency Ω_m .

Linearizing the equations of motion (3.3) with respect to α , against the background of the ground state (3.22), and assuming that $\alpha, \alpha^* \sim \exp(-i\Omega t)$, we obtain a set of algebraic equations which are homogeneous in α, α^* . The condition that these equations are consistent, determines the frequency and damping of the collective oscillations:

$$\Omega_m = -i\gamma \pm \sqrt{4S_m(2T_m + S_m)N_1^2 - \gamma^2}. \quad (4.10)$$

This formula leads to the important conclusion that the criterion for internal instability on the m -th collective mode is independent of the amount of damping and is determined, just as in the conservative case, by the condition

$$S_m(2T_m + S_m) < 0. \quad (4.11)$$

Within the framework of the S theory, the collective oscillations of a system of parametric spin waves are spatially homogeneous. When spatial dispersion is taken into account, each normal mode corresponds to a whole branch of $\Omega_m(\kappa)$, where (4.10) defines the gap. Spatially-inhomogeneous collective oscillations $\delta_n, \delta_\psi \sim \exp[i(\kappa r - \Omega_m t)]$ have a definite analogy with second sound. In contrast to the usual second sound, a gas of thermal magnons in a system of parametric waves exhibits oscillations not only in the number n_k of pairs, but in their phase ψ_k as well.

The spectrum $\Omega_m(\kappa)$ of these waves is investigated in^[49]. In the simple case when $\kappa \parallel M$,

$$\Omega_m(\kappa) = -i\gamma \pm \sqrt{\left[2(T_m + S_m)N_1 + \omega'' \frac{\kappa^2}{2} \right]^2 - 4T_m^2 N_1^2 - \gamma^2},$$

where $\omega'' = \partial^2 \omega / \partial \kappa^2$. Possible forms of the function $\Omega_m(\kappa)$ (with $\gamma = 0$) are shown in Fig. 9. The region of negative values corresponds to the instability of the ground state. We note that, for large κ , collective oscillations are always damped, i.e., $\Omega_m(\kappa) = -i\gamma + (\omega'' \kappa^2 / 2)$.

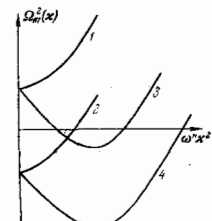


FIG. 9. Possible variants of the collective oscillation spectrum ($\gamma = 0$). For $\Omega^2 < 0$ the ground state is unstable. Curves 1 and 2 correspond to $T_m + S_m > 0$; curves 3 and 4 correspond to $T_m + S_m < 0$.

(b) Resonance excitation of collective oscillations. The collective oscillations discussed above are seen experimentally as low-frequency ($\Omega \approx \text{sec}^{-1}$) oscillations of the longitudinal magnetization M_z . Pulsed excitation of these oscillations can frequently be observed during the transient state after the end of the pump pulse.

The resonance method is the most convenient way of exciting collective oscillations. The procedure is to apply to the ferromagnet both the pump field $h(t) \sim e^{-i\omega_p t}$ and a weak field $h_s \parallel M$ with frequency close to ω_p , i.e., $\omega_s = \omega_p + \Omega^{[27]}$. Calculations reported in, [27] based on the equations of motion (3.3), show that the susceptibility $\chi''_{\omega_p + \Omega}$ resonance frequencies, namely, $\Omega = \pm \Omega_0$ which coincide, as expected, with the natural frequency of the zero mode, Ω_0 , in the absence of damping:

$$\chi''_{\omega_p + \Omega} = \chi'' \left(\frac{h}{h_1} \right)^2 \frac{2\gamma^2 [\Omega_0^2 + \Omega^2 + 4\Omega(T_0 + S_0)N]}{(\Omega_0^2 - \Omega^2)^2 + 4\gamma^2\Omega^2} .$$

For large excesses above the threshold, when $\Omega_0^2 \gg \gamma^2$, the line shape is nearly Lorentzian, with width equal to the spin-wave damping γ . At resonance, the susceptibility is given by

$$\chi''_{\omega_p + \Omega_0} = \chi'' \left(\frac{h}{h_1} \right)^2 \left[1 \pm \sqrt{1 + \frac{T_0^2}{S_0(2T_0 + S_0)}} \right] . \quad (4.12)$$

The fundamental point is that the susceptibility may turn out to be negative. This corresponds not to absorption but to amplification of the weak signal. It follows from (4.12) that absorption occurs at the frequency $\omega_p + \Omega$, and amplification at the mirror frequency $\omega_p - \Omega$.

The appearance of amplification can be regarded as a consequence of decay instability of the ground state (with the "slow" frequency equal to zero) into electromagnetic radiation (with slow frequency Ω) and a collective oscillation with characteristic frequency Ω_0 . The law of conservation of energy in this process is $0 \rightarrow \Omega + \Omega_0$. Amplification therefore occurs at the frequency $-\Omega_0$, which corresponds to (4.12). In this language, absorption is a consequence of the decay of the weak signal into the ground state and the collective mode with the conservation law $\Omega = 0 + \Omega_0$.

The collective resonance was observed experimentally in [27] in single-crystal YIG. Good quantitative agreement between theory and experiment was noted. In particular, the dependence of the susceptibility to a weak signal on the pump power (Fig. 10) was found to be in good agreement with (4.12) right up to the first threshold $(h/h_1)^2 = 8 \text{ dB}$. It was also noted that the collective resonance can be used as a convenient and relatively simple method of measuring the spin-wave relaxation time. Measurements show that, in accordance with the theory, the resonance absorption linewidth is practically independent of the pump power, and is in good agreement

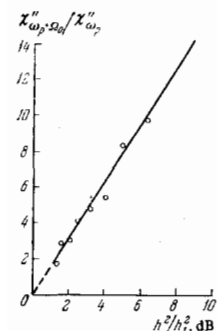


FIG. 10. Measured susceptibility for a weak signal as a function of pump power (YIG sphere, $M \parallel (100)$).

with the values of γ obtained from the threshold for parallel excitation [27].

(c) Auto-oscillations of magnetization. It is well known that, in the case of parametric generation of spin waves, the stationary state is frequently not established, and the magnetization executes complicated auto-oscillations about some mean value.

The main experimental facts on these auto-oscillations, obtained for high-quality YIG crystals under parallel excitation are as follows [37, 50, 51]:

(1) The auto-oscillation frequencies lie in the range between 10^4 and approximately 10^7 Hz (depending on the pump power and the constant magnetic field). For a small excess above the threshold, the auto-oscillation spectrum consists of a single line. As the power level increases, there is an increase in the number of lines which also shift toward higher frequencies. For large excesses above the threshold, noise-type spectrum is observed.

(2) The threshold for auto-oscillations is usually very low: 0.1–1 dB relative to the parametric excitation threshold, with the exception of small wave vectors ($H > H_C$) where the auto-oscillation threshold is appreciably higher. The threshold also rises when internal inhomogeneities are introduced into the crystals [52].

(3) Giant crystallographic anisotropy in auto-oscillation properties, which substantially exceeds the anisotropy in the spin-wave spectrum, has been observed. Thus, the auto-oscillation intensity in YIG when the magnetization lies along the $\langle 111 \rangle$ axis exceeds the intensity for the $\langle 100 \rangle$ axis by a factor of roughly 100.

The physical nature of these auto-oscillations is one of the basic problems for the parametric excitation of spin waves.

Various hypotheses have been put forward in this connection. The simplest hypothesis [53] is that several discrete frequencies corresponding to the natural oscillations of the crystal are present in the spectrum of parametrically excited spin waves. Beats between these frequencies lead to the appearance of the auto-oscillations. This hypothesis explains [53] a number of experimental facts (the dependence of the auto-oscillation frequency on the magnetic field and the crystallographic orientation of magnetization), but it totally ignores the dependence of the auto-oscillation frequency on the pump power, and the question of the origin of the few discrete frequencies. We note that the S-theory predicts the existence of the single frequency $1/2\omega_p$ in the stationary state.

Another group of hypotheses is based on the effect of excited waves on magnetization (see, for example, the paper by Green & Schlömann [54]). If the mean magnetization of the crystals follows the amplitude of the spin waves with a certain delay, then the auto-oscillations in magnetization may build up in the crystal. Monosov's monograph [37] is written from this point of view and is based on the phenomenological equations of Bloch and Bloembergen. In fact, however, the appearance of the auto-oscillations can be influenced only by the inertia of the thermal spin waves with frequency of the order of ω_p . This problem should be solved with the aid of the kinetic equation for the waves. So far, it has not been solved. Nevertheless, it might be expected that, in most experimental situations, the effect of inertia can be neglected.

The auto-oscillations find a natural explanation within the framework of the S-theory as the result of the instability of the stationary state against the excitation of collective oscillations, which was described in Sec. 4(a). If the instability conditions $S_m(2T_m + S_m) < 0$ are satisfied for at least one mode (of number m), the system of parametrically excited spin waves has no stable stationary state within the framework of the S theory. There are then two conceivable possibilities: either the system is brought out of the region within which S theory is valid (this should be accompanied by a strong increase in the amplitude of the excited waves), or the oscillations should settle down around the stationary state. These oscillations (if they develop) are observed experimentally as auto-oscillations of magnetization. General considerations suggest that the auto-oscillations may be both regular and random. In the latter case they can be looked upon as "secondary" turbulence with time scale much greater than the scale of the "main" turbulence (the period of the spin waves).

It is clear from (4.10) that the instability of the stationary state is purely aperiodic ($\text{Re } \Omega_m = 0$) and, therefore, the secondary turbulence is strong. This means that the analytic solution for the nonlinear stage of development of collective instability and the description of secondary turbulence (if it appears) are extremely difficult to obtain. Computer simulation of secondary turbulence would therefore seem to be useful. This however requires an inordinate amount of machine time and is hardly practicable in a real situation, for example, in YIG. This forces us to turn again to a numerical experiment, using simple models of the ground state.

A numerical experiment on the excitation of auto-oscillations was described in^[28]. It was based on the two-beam model in which it was assumed that the spin waves were localized around two fixed angles $\theta_1 = 1/2\pi$, $\theta_2 = 1/4\pi$. The coefficients S_0 and P_0 were chosen to be close to those calculated for YIG, with the magnetic field along the $\langle 111 \rangle$ axis (see below), so that the instability conditions were satisfied for the zero mode.

The numerical experiment showed that steady auto-oscillations of amplitudes and phases were established in this model (Fig. 11). The dependence of the frequency in these auto-oscillations on the pump level is qualitatively in agreement with the analogous result usually observed experimentally. The above model was also used to carry out an experiment simulating the development of collective instability for $m \neq 0$. The behavior of the resultant amplitude during the nonlinear stage of development of the instability was investigated. This is interesting because there is no change in the resultant amplitude during the linear stage. We chose beams with $\theta_1 = \theta_2 = 1/2\pi$ and $\varphi_2 = \varphi_1 + 1/2\pi$. The experiment showed (Fig. 12) that states were established in which both the sum and the difference of the wave amplitudes underwent oscillations. The oscillations in the amplitudes appear as a result of the interaction between collective modes with different m .

The numerical experiment based on the above models thus shows that, within the framework of the S theory, the development of the internal instability of the ground state does indeed lead to auto-oscillations. The properties of these auto-oscillations, i.e., the dependence of frequency and spectral composition on the pump power, are comparable with the properties of auto-oscillations observed in laboratory experiments. Thus, both numeri-

FIG. 11. Time dependence of pair amplitude along beams for the $m = 0$ mode instability. N_1 and N_2 represent the two beams with $\theta = 1/2\pi$ and $\theta = 1/4\pi$.

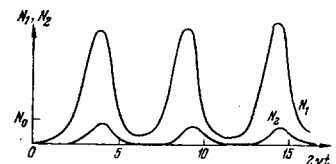
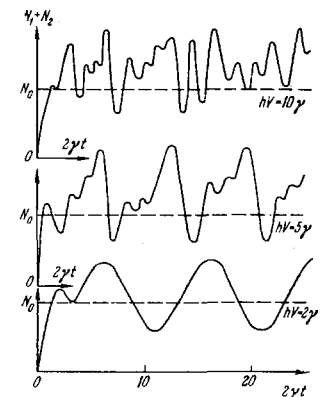


FIG. 12. Time dependence of resultant pair amplitude along the beams for the $m = 2$ mode instability.



cal and laboratory experiments show that the development of auto-oscillations has no substantial effect on the mean level of parametrically excited waves. The numerical experiment shows moreover that, during the development of instability, the zero mode pronounced oscillations in the resultant amplitude. Smaller oscillations in the resultant amplitude which are accompanied by a reduction in the measured χ'' are found for higher-mode instabilities. It is interesting that the appearance of the auto-oscillations in the numerical experiment is usually accompanied by a reduction in mean value of χ' . This has also been observed in laboratory experiments.

The above result can be used to predict situations in which auto-oscillations should be observed in a real experiment. We have calculated S_m and T_m for YIG using (4.5)–(4.8) for a typical experimental situation: $N_2 = 1/3$ (sphere), $\omega_p = 9.4$ Hz, $k = 0$ ($H = H_C$), $\omega_M = 4.5$ Hz, $\omega_a = 0.23$ Hz (room temperature) (Table II).

It is clear that not only the magnitudes but also the signs of the coefficients depend on the direction of magnetization. Substituting the tabulated data in the instability criterion (4.11), we can readily verify that in the "easy" direction $\langle 111 \rangle$ we have an instability for the zero mode, whereas in the "difficult" direction $\langle 100 \rangle$ all the modes are stable in this situation. In the experiment with $H = H_C$, in the difficult direction the auto-oscillations are in fact absent up to $h_2 \approx 6-7$ dB, which corresponds to the second threshold. On the other hand, in the "easy" direction there are strong auto-oscillations virtually immediately after the threshold h_1 ^[37].

The condition for the appearance of the auto-oscillations in different experimental situations was analyzed in detail in^[55] where use was made of the graphical representation of the instability criterion (4.11) in the form of a phase diagram. Using the expressions for S_0 and T_0 given by (4.5)–(4.7), we can construct the lines $S_0 = 0$ and $2P_0 + S_0 = 0$ on the ω_p/ω_M , N_{z0} plane, which represents the boundaries of the instability region for the zero mode (Fig. 13). The unstable "phase" lies between these curves. Similarly, one can construct phase diagrams on the ω_p/ω_M , N_{z2} plane, which represent the instability regions for the $m = 2$ and $m = -2$ modes (Fig. 14).

TABLE II. The Coefficients S_m and T_m in units of $2\pi g^2$ for YIG

Orientation	T_0	S_0	$T_2 = T_{-2}$	S_2	S_{-2}
(100)	0.28	0.52	0.11	0.04	-0.36
(111)	-0.75	0.30	0.05	0.01	-1.27

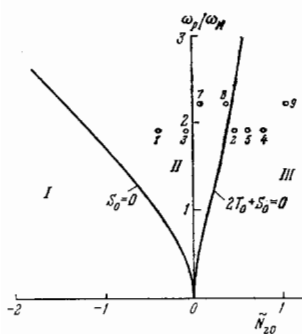


FIG. 13

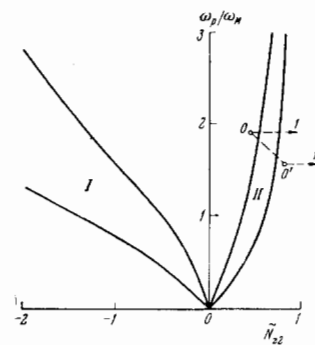


FIG. 14

FIG. 13. Phase diagram for the $m = 0$ mode. Regions I and III correspond to the stable phase; strong auto-oscillations develop in region II.

FIG. 14. Phase diagrams for the $m = 2$ and $m = -2$ modes. The $m = 2$ mode is stable in region I and the $m = -2$ mode in region II.

By varying the experimental conditions, for example, by varying the temperature, the specimen shape, and so on, it is possible to move the point on the phase diagram corresponding to the given experimental situation and, in the course of this, the boundaries of the instability region may be intersected.

In an experiment in which measures have not been taken to increase the sensitivity, one usually observes the only zero-mode instability which leads to very strong auto-oscillations of magnetization. The results of such experiments ($\omega_p = 9.4$ Hz and $T = 300^\circ\text{K}$) with pure YIG single crystals and YIG crystals doped with scandium (which reduces the anisotropy field) are summarized in Table III.

The phase diagram in Fig. 13 shows points representing the experimental situations defined in Table III. It is clear that strong auto-oscillations are observed in those and only those situations where the representative point enters the instability region. It is interesting that points 2 and 8 lie near the instability boundary and cut this boundary after a small change in the temperature. For example, for point 2 calculations show that this occurs for $T \approx 330^\circ\text{K}$, whereas experiment shows that the oscillations occur for $T \gtrsim 360^\circ\text{K}$.

Experiments performed with increased sensitivity showed the presence of weak auto-oscillations in those cases where the theory predicts instability for the $m = -2$ mode and stability for the $m = 0$ mode^[55]. Figure 15 shows the dependence of the threshold for weak auto-oscillations on the constant magnetic field for this particular experimental situation. It is clear that the auto-oscillations appear in two magnetic-field intervals. The appearance of the auto-oscillations in region I is explained in a natural fashion by the phase diagram which shows the instability region for $m = -2$ (Fig. 14). This diagram gives the trajectory of the representative point as the magnetic field is varied. The initial point O, which corresponds to $k = 0$ ($H = H_C$), lies in the stable region. As H is reduced, the wave number increases,

TABLE III

Crystal	$\text{YIG}: \frac{\omega_p}{\omega_M} = 1.9, \frac{\omega_a}{\omega_M} = 0.05$						$\text{YIG + Sc}: \frac{\omega_p}{\omega_M} = 2.2, \frac{\omega_a}{\omega_M} = 0.005$		
	1 0	2 0	3 1/3	4 1/3	5 1	6 1	7 0	8 1/3	9 1
No. of expt. Demagnetizing factor (N_d)	(111)	(100)	(111)	(100)	(111)	(100)	(100)	(100)	(100)
Orientation of magnetization	Yes	No	Yes	No	No	No	Yes	Yes	No
Strong auto- oscillations									

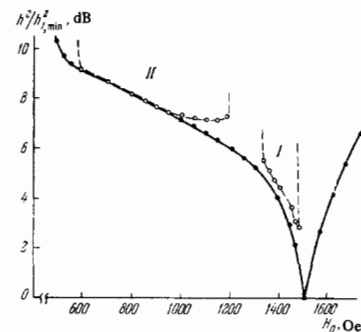


FIG. 15. Weak auto-oscillation threshold vs. constant-magnetic field (YIG sphere, $M \parallel (100)$).

and the $0 \rightarrow 1$ trajectory cuts the stability region. The theoretical width of the instability region for YIG at room temperature is 350 Oe. The experimental width of region I in Fig. 15 varies somewhat with the shape and size of the specimen and lies in the range 150–250 Oe. The width of this region decreases with decreasing temperature, and disappears altogether at temperatures below 275°K . This is explained by an increase in anisotropy and magnetization, which shifts the initial point on the phase diagram along the 00 line (Fig. 14). It is clear that the trajectory corresponding to changes in H at low temperatures does not cut the instability region for the $m = -2$ mode.

Auto-oscillations in region II in Fig. 15 have a more complicated origin. The limits of this region coincide with the field interval in which one observes hard parametric excitation of spin waves due to negative non-linear damping (sec. 5). The conditions for the appearance of these auto-oscillations are analyzed in^[46] in terms of the kinetic equation.

In conclusion, we must recall that the simple theory of auto-oscillations discussed in this section predict that the threshold h_a for the auto-oscillations coincides with the parametric excitation threshold h_1 and that the frequency of the auto-oscillations is zero for $h = h_a$. Experiment shows, however, a finite threshold for the auto-oscillations and a nonzero initial frequency. In single-crystal YIG, the threshold for the auto-oscillations is usually 0.1–1 dB, and the initial frequency does not correlate with the size of the threshold and varies in the range 10^4 – 10^5 Hz,^[37, 51] depending on the constant magnetic field. These facts can be explained by the influence of weak nonlinear damping which has no substantial effects on the magnitudes of χ' and χ'' , by the presence of random inhomogeneities in the crystals^[49], by the absence of exact axial symmetry, by the reaction of the specimen on the resonator^[56], and so on. Further theoretical and experimental studies of the auto-oscillations will be necessary to establish the relative contributions of these mechanisms.

5. OTHER PROBLEMS IN SPIN-WAVE TURBULENCE.

(a) Effect of random inhomogeneities. The elementary theory of the nonlinear stage of parametric excitation of waves (the S theory) described above is only the first important step along the way to an understanding of the phenomena which occur in real crystals during parametric resonance. A relatively large volume of data has now accumulated on the way in which parametric excitation of waves is affected by factors which have not been taken into account in the simple S theory. These results were obtained with the aid of a formalism which is occasionally quite complicated and cannot therefore be outlined in the present review to the same degree of completeness as the S-theory. The present section is concerned with a very brief review of these results, and most of the material is theoretical. Experimental studies of phenomena outside the framework of the S theory are only just beginning.

We start with the influence of random magnetic inhomogeneities on the parametric excitation of waves.

With very rare exceptions, real ferromagnets contain various types of magnetic inhomogeneities, including random distributions of magnetic ions over the crystal lattice sites, impurities, nonmagnetic inclusions, surface roughness, polycrystalline structure, and so on. These inhomogeneities are known to lead to the very effective two-magnon relaxation process which conserves the frequency but not the momentum of the magnons. The nature of the magnetic inhomogeneities and their influence on the ferromagnetic resonance linewidth were investigated extensively in many papers (see, for example, the monograph by Sparks^[57] and the paper by Schlömann^[60] in the case of unstable homogeneous second-order precession. In this case, the frequency of homogeneous precession is equal to the frequency of parametric spin waves, and the spin waves which arise as a result of the two-magnon relaxation of homogeneous precession ($\omega_0 \rightarrow \omega_{\mathbf{k}}$) are involved in the four-magnon parametric process ($2\omega_0 \rightarrow \omega_{\mathbf{k}} + \omega_{-\mathbf{k}}$) as well. Parametric waves therefore reach a substantial excitation level and produce an effective reaction on the homogeneous precession even before the instability threshold. This phenomenon leads to a "spread" in the threshold even in the case of a small number of inhomogeneities.

In the case of unstable homogeneous first-order precession and parallel excitation, the frequency of the parametric spin waves is equal to one half of the pump frequency and there is no spread in the threshold. This does not mean, however, that inhomogeneity has no effect on the threshold or the behavior of spin waves beyond the threshold.

The effect of inhomogeneities on parallel excitation is discussed in a large number of experimental papers^[61]. The experiments were largely performed on polycrystals. They showed that a reduction in grain size to a value of the order of the parametric wavelength leads to a substantial increase in the threshold. The results are usually treated in terms of simple representations: the parallel excitation threshold is determined from the formula

$$h_1 | V_{\mathbf{k}} | = \gamma_{\mathbf{k}} + \gamma_{\text{imp}}, \quad (5.1)$$

where γ_{imp} is the damping rate for the spin wave due to scattering by grain boundaries and $\gamma_{\mathbf{k}}$ is the damping rate due to intrinsic relaxation processes.

Sparks' book^[57] contains a criticism of this approach,

which can be summarized as follows. Two-magnon processes do not remove energy from the parametric-wave system and, therefore, the energy balance condition for them has the same form as before, i.e., (2.22), but this condition takes into account only the intrinsic damping $\gamma_{\mathbf{k}}$. However, the effect of the inhomogeneities is that the normal modes are no longer plane waves, but some linear combinations of them, and these are in fact excited by the pump. To determine the threshold, one must obviously average the balance condition (2.22) over the waves which make up the normal mode with the minimum threshold. In our notation, the Sparks threshold formula takes the form

$$h_1 \int |V_{\theta}| N_{\theta} \sin \theta d\theta = \int \gamma_{\theta} N_{\theta} \sin \theta d\theta. \quad (5.2)$$

It predicts that h_1 is a slow function of the inhomogeneity density. In fact, in the limiting case of a highly inhomogeneous medium, the parametric waves fill the entire resonance surface $\omega_{\mathbf{k}} = 1/2\omega_p$ uniformly. It then follows from (5.2) that

$$h_1 \int V_{\theta} \sin \theta d\theta = \int \gamma_{\theta} \sin \theta d\theta. \quad (5.3)$$

Substituting $\gamma_{\theta} = \text{const}$ and V_{θ} from (2.26) for isotropic ferromagnets, we obtain $h_1 = 3V/2\gamma$, i.e., there is an increase by a factor of 1.5 in the threshold as compared with the homogeneous case.

The threshold for the parametric excitation of spin waves in a medium with random inhomogeneities is discussed in^[34] subject to the approximation $\gamma_{\text{imp}} \ll \omega$. It is shown that the inhomogeneities not only spread out the pair distribution function, but violate the strict phase correlations within each pair: $\langle \bar{c}_{\mathbf{k}} \bar{c}_{\mathbf{k}}^* \rangle > \langle c_{\mathbf{k}} c_{-\mathbf{k}}^* \rangle$ (the bar represents averaging over the impurity ensemble). This weakens the interaction between the spin waves and the pump, and leads to an additional increase in the threshold over and above the increase predicted by the Sparks formula (5.2). For low impurity densities ($\gamma_{\text{imp}} \ll \gamma$), the spread is $\Delta\theta \approx (\gamma_{\text{imp}}/\gamma)^{1/2}$, and the threshold is

$$h_1 V_1 \approx \gamma + \frac{\gamma_{\text{imp}}}{2\sqrt{2}} \ln \frac{\gamma}{\gamma_{\text{imp}}}. \quad (5.4)$$

The logarithm in this formula appears because loss of energy from the equator becomes important in this limit as a result of the two-magnon scattering.

When $\gamma_{\text{imp}} \gg \gamma$, the distribution N_{θ} clearly becomes isotropic, and the threshold amplitude is determined from the expression

$$h_1^2 \int_0^{\pi/2} V_{\theta}^2 \sin \theta d\theta = \gamma \gamma_{\text{imp}}. \quad (5.5)$$

Therefore, the magnitude of h_1 in this case is greater by a factor of $(\gamma_{\text{imp}}/\gamma)^{1/2}$ than predicted by (5.3) because the latter does not take into account the violation of the phase correlation. When (5.4) and (5.5) are compared with experiment, it must be remembered that they are not valid if the size of the inhomogeneities is much greater than the spin wavelength.

The post-threshold behavior of spin waves in a ferromagnet with random inhomogeneities is also discussed in^[34] within the framework of the S-theory. The inhomogeneities lead to an increase in the stationary level of wave limitation by a factor of $n_{\mathbf{k}} b \gamma_{\text{imp}} / \gamma$. This effect is also explained by a reduction in the pair phase correlation due to the two-magnon scattering. The quantity $\sigma_{\mathbf{k}}$ is not substantially altered because the amplitude limitation conditions for large excesses above the

threshold $|p| \ll hV$ remains in force even in the presence of inhomogeneities. This ensures that the nonlinear susceptibilities given by (2.33) and (2.34) are not very sensitive to inhomogeneity density. A serious comparison between the conclusions given in^[34] and experimental data has not as yet been carried out.

(b) Initiation and fine structure of parametric turbulence. All real systems exhibit thermal fluctuations, and there is considerable interest in their behavior during parametric excitation of waves. It is clear that, as the instability threshold is approached, there is an increase in the level of fluctuations in the system. Beyond the instability threshold there are at least two possible cases: either the fluctuations in the region of \mathbf{k} space near the instability wave vector \mathbf{k}_0 increase to the macroscopic level, in which case a wave packet is produced with a certain width κ , or we have a state which is singular in \mathbf{k} and the fluctuations become frozen at a certain level. The appearance of the singular state can be compared with a phase transition of the second kind, for example, condensation of a Bose gas, or a transition to the superconducting state.

A phase transition is a change in the state of a system due to its instability for $T < T_1$, where T_1 is the transition temperature. This results in the appearance of long-range order in the system, and the order parameter is a function of temperature of the form $(T_1 - T)^{1/2}$. When a stationary spectrum is established in the form of one angular pair of waves against the background of fluctuations, we again observe long-range order, i.e., the phase coherence of waves forming the pair. If we continue this analogy with phase transitions, we can compare the pair amplitude with the order parameter, and the temperature with the pump power. Near the phase transition, the fluctuations also undergo a rapid increase and it is precisely the behavior of fluctuations for $T \rightarrow T_1$ which determines whether or not the phase transition will take place.

We shall now describe the behavior of fluctuations during the parametric excitation of waves. Well away from the excitation threshold ($hV_{\mathbf{k}} < \gamma_{\mathbf{k}}$) the fluctuations can be described in terms of the linear approximation. The pump field produces a deviation of the wave distribution function $n_{\mathbf{k}}$ from the thermodynamic equilibrium value $n_{\mathbf{k}}^0$:

$$\Delta n_{\mathbf{k}} = n_{\mathbf{k}} - n_{\mathbf{k}}^0 = n_{\mathbf{k}}^0 \frac{|hV_{\mathbf{k}}|^2}{[\omega_{\mathbf{k}} - (\omega_p/2)]^2 + v_{\mathbf{k}}^2}, \quad (5.6)$$

where

$$v_{\mathbf{k}}^2 = \gamma_{\mathbf{k}}^2 - |hV_{\mathbf{k}}|^2. \quad (5.7)$$

The formula given by (5.6) may be regarded as the resonant response of the system under the conditions of parametric excitation to a random Langevin force which represents the interaction between the system and the thermostat. Thus, the application of the pump and the random force results in the appearance of a wave packet with maximum at $\omega_{\mathbf{k}} = 1/2\omega_p$ and frequency width $v_{\mathbf{k}}$. It is clear that as $hV_{\mathbf{k}} \rightarrow \gamma_{\mathbf{k}}$, the distribution width $v_{\mathbf{k}} \rightarrow 0$ and the integrated fluctuation intensity in a particular direction increases as $v_{\mathbf{k}}^{-1}$, where v_{Ω} is the value of $v_{\mathbf{k}}$ on the resonance surface.

The behavior of the fluctuations near the threshold and when $hV_{\mathbf{k}} > \gamma_{\mathbf{k}}$ must be described by the nonlinear equations. It is shown in^[62] that the character of the "phase transition" is very dependent on the quantity δ ,

i.e., the dimensionality of the distribution $n_{\mathbf{k}}$ in the ground state of the S-theory. When $\delta = 0$, the waves are located at a pair of points, and when $\delta = 1$, they lie on a line (this case is usually realized in isotropic ferromagnets). Finally, when $\delta = 2$, they lie on a surface in the \mathbf{k} space.

The singular distribution of parametric waves, which appears for $h > h_1$, modifies the fluctuation damping rate in the neighbourhood of the resonance surface. It turns out that in the diagonal-Hamiltonian approximation the fluctuation intensity is given by (5.6) as before, except that $\omega_{\mathbf{k}}$ is now replaced by $\tilde{\omega}_{\mathbf{k}}$ and $hV_{\mathbf{k}}$ by $P_{\mathbf{k}}$. In the linear approximation, their contribution to the renormalization of frequency and pump need not be taken into account. It is then clear that $v_{\Omega} = 0$ at those points on the resonance surface where the parametric-wave amplitudes are nonzero. In the neighborhood of these points

$$\Delta n_{\mathbf{k}} \sim \frac{1}{V_g^2 \kappa_{\perp}^2 + (1/2) v_{\perp}^2}, \quad (5.8)$$

where V_g is the group velocity and κ_{\perp} and κ_{\parallel} are the deviations of the wave vector \mathbf{k} across and along the resonance surface respectively.

The spread in the singular distribution will obviously occur for $\delta = 2$ or 1 if the integrated fluctuation intensity given by (5.8) becomes infinite. This formula is then no longer valid, and we must take into account the contribution of fluctuations to the self-consistent pump and the renormalization of the frequency.

When $\delta = 2$ the integral converges as κ_{\parallel}^{-1} . Calculations show that this is accompanied by the establishment of the Lorentz distribution $n_{\mathbf{k}}$, the width of which $\nu = \kappa_{\parallel} V_g$ decreases with increasing excess above the threshold. At the threshold $\nu = \xi^{1/2} \gamma$ where $\xi = (2\pi)^2 k_0^2 S n_{\mathbf{k}}^0 V_g^{-1}$ is a small parameter characterizing the effect of thermal fluctuations. Order-of-magnitude calculations show that $\xi \approx l_{\mathbf{k}_0} (T/T_c) \sim 10^{-2} - 10^{-3}$. In these expressions l is the lattice constant and T_c is the Curie temperature. For excesses above the threshold that are not too small $h - h_1 > h_1 \xi^2$, we have

$$\frac{\nu}{\gamma} = \xi \frac{h_1}{\sqrt{h^2 - h^2}}.$$

When $\delta = 1$, the thermal fluctuation divergence is logarithmic, and the distribution width ν is exponentially small^[62]. The integrated fluctuation intensity is finite for one pair ($\delta = 0$) and it is only in this case that one might hope for the appearance of a state which is singular in \mathbf{k} in the presence of thermal fluctuations. However, calculations show^[62, 63] that these hopes are unjustified because, as a rule, the ground state is unstable against the excitation of spatially-inhomogeneous collective oscillations. The nonlinear stage of development of this instability will be described in the next section.

It is important to note that, in addition to the broadening in \mathbf{k} , the distribution function for the parametric waves has a finite spectral width $\Delta\omega$. In the diagonal-Hamiltonian approximation^[33]

$$\Delta\omega = \frac{v_{\mathbf{k}}^2}{\gamma}.$$

The multifrequency character of parametric turbulence is a consequence of the fact that the Langevin random force to which the parametric waves are the response has a broad frequency spectrum. However, all this is

valid only so long as we need not take into account the nondiagonal terms of the Hamiltonian which have been neglected and which were shown in^[33] to lead to a substantial change in the random-force spectrum. In particular, in addition to the Langevin random-force $f_L(k)$ with a white spectrum there is an additional random force $f_k(k, \omega)$ with a narrow spectrum whose width is of the order of the spectral width of the parametric wave packet, $\Delta\omega$, and a maximum at the frequency $1/2\omega_p$. The square of its amplitude is proportional to $SN^3/\Delta\omega$ where N is the integrated wave intensity. At a certain critical pump amplitude

$$h^* - h_1 \approx h_1 \xi^{3/5} \left(\frac{\omega}{\gamma} \right)^{1/5} \approx 10^{-2} h_1$$

the "intrinsic" noise level f_S is comparable with the thermal noise level f_L^2 . When $h > h^*$, the system of parametric waves becomes unstable against the "buckling" of the frequency spectrum. In fact, a random reduction in the spectral width $\Delta\omega$ of the packet gives rise to a narrowing of the spectrum of the random force f_S and an increase in its amplitude. This enhances the reduction $\Delta\omega$, as a result of which the force f_S becomes even "narrower and stronger" and so on. The contraction process continues so long as the distribution widths of these parametric waves and of the intrinsic noise spectrum do not vanish. This process cannot occur in the direction of increasing widths of these distributions. This is prevented by the resonance character of the effect of the pump.

We thus see that, when $h = h^*$, we have a phenomenon which is analogous to a phase transition, i.e., the appearance of a "condensate." A new packet of waves appears against the background of the above multifrequency parametric turbulence, with the same spread in k but oscillating at the strictly fixed frequency $1/2\omega_p$. Analysis of this transition is a very complicated task. It may be that this is a phase transition of first order but close to second, i.e., when $h = h^*$ the single-frequency turbulence appears suddenly, but the size of this jump is small. When $h > h^*$ the amplitude of the single-frequency part of the turbulence N_S is found to increase, rapidly reaching the asymptotic value given by the S theory:

$$SN_S \approx \sqrt{h^2 V^2 - \gamma^2},$$

whereas the multifrequency part rapidly decreases and may be looked upon as fluctuations against the background of the single-frequency turbulence. The spectral width of these fluctuations is of the order of

$$\Delta\omega = \frac{\nu^2}{\gamma} \approx \nu \left(\frac{\gamma}{k_0 V_g} \frac{h^2 - h_1^2}{h_1^2} \right)^{2/3}.$$

Here ν is the width of the distribution over the natural frequencies on both the multi- and single-frequency parts of the turbulence.

In addition to fluctuations at frequencies close to $1/2\omega_p$ there are also fluctuations due to thermal excitation of collective oscillations (cf. section 4(a)), which lie at frequencies separated from $1/2\omega_p$ by an amount of the order of $SN_S \gg \Delta\omega$.

The above picture of the initiation of single-frequency turbulence refers only to the case where the ground state is stable against the excitation of collective oscillations. It is well-known that, in the opposite case, auto-oscillations are produced and can be looked upon as giant fluctuations, destroying the single-frequency turbulence and leading to strong multi-frequency turbulence

with the spectral width of the order of SN_S which is equal to the width of the region excited in k space.

(c) Strong turbulence and self-focusing of narrow parametric-wave packets. We shall now consider the situation where the excitation threshold is a minimum for a single pair of waves. This occurs, for example, when spin waves are excited by homogeneous precession in the case of second-order instability ($2\omega_k = 2\omega_p$) and for parallel excitation in uniaxial ferromagnets with "easy plane" anisotropy. It follows from the S theory (see^[20]) that, in this case, a monochromatic standing wave which is coherent throughout the crystal will be excited below the second threshold. This wave can be used to amplify and excite hypersonic waves, to modulate light, and so on. However, a necessary condition for the realization of the single-mode state is that it must be stable. In the nondecay part of the spectrum the main processes leading to instability are the following four-wave processes^[62, 63]:

$$2\omega_{\pm k_0} = \omega_{\pm k_0 + \mathbf{x}} + \omega_{\pm k_0 - \mathbf{x}}, \quad (5.9)$$

$$\omega_{k_0} + \omega_{-k_0} = \omega_{k_0 + \mathbf{x}} + \omega_{k_0 - \mathbf{x}}. \quad (5.10)$$

The process defined by (5.10) describes the interaction of pairs and corresponds to the diagonal Hamiltonian (3.1). The process defined by (5.9) defines the instability of one wave and was previously ignored on the ground that in the case of a large number of waves it has a high threshold because of the randomization of the individual phases.

The instability growth rate for the processes (5.9) and (5.10) is very dependent on the sign of the coefficients S and T of the Hamiltonian. For small κ we must have $S > 0$ and $T > 0$ for stability. However, even when these conditions are satisfied, perturbations with $\kappa \approx \kappa_0$ may turn out to be unstable, where

$$\omega'' \kappa_0^2 = \sqrt{(hV)^2 - \gamma^2}. \quad (5.11)$$

To ensure stability for these values of κ , we must satisfy the additional requirement $0 < hV - \gamma \lesssim \gamma(\gamma/\omega)^2(S/T)^{1/4}$ which defines a very narrow interval of pump intensities h .

The nonlinear stage of development of the instability of one pair was investigated in^[64, 65]. The basic feature of this problem is the narrowness of the wave packets excited in k space, which has meant that the problem could be described in the language of wave envelopes. The simplest variant of the nonlinear behavior of the system is its transition into one of the possible stationary states which take the form of a periodic modulation wave $A(r - Vt)$, which is either at rest or moves with constant velocity. Analysis of the stability of such waves in the case of small modulation depth suggests that all the stationary states are unstable and, therefore, the nonlinear behavior of the system is essentially non-stationary. Such a state is highly turbulent and can be represented by a stochastic superposition of envelopes propagating mainly in the direction perpendicular to k_0 . The modulation depth is of the order of unity, and the characteristic wavelength is $\sim \kappa_0^{-1}$. The average level of the resulting turbulence turns out to be of the order of the pair amplitude in S theory. The modulation picture changes substantially over a period of the order of $[(hV)^2 - \gamma^2]^{1/2}$.

An interesting phenomenon occurs against the background of this turbulence, namely, the collapse of the standing-wave envelopes. It turns out that deep modulations $A(r, t)$ are not dissipated but contract in such

a way that the amplitude at the center of the packet rises rapidly and is restricted by the nonlinear damping to a level much higher than the mean turbulence level. This can be compared with self-focusing in nonlinear media in optics, which in certain cases leads to the collapse of a beam in a finite time^[66, 67].

Computer calculations show^[65] that, when the excess above the threshold is small, these collapse regions are practically unnoticeable, and for $h \gtrsim 3h_1$ practically every amplitude maximum with collapse. The energy dissipation in these collapses leads to an effective nonlinear damping described by $\gamma(N) \approx \gamma + \eta N$, $\eta \approx |S|$.

A promising experimental method of studying strong turbulence is measurement of the spectral density of electromagnetic radiation emitted by a ferromagnet at frequencies around ω_p and $1/2\omega_p$. In the absence of the collapses, the spectral width of the emission is $\sim [(hV)^2 - \gamma^2]^{1/2}$. The appearance of collapses, on the other hand, is accompanied by a substantial broadening of the emission spectrum, which can probably be used as a means of detection.

6. CONCLUSION

The results summarized in this review show that substantial progress has now been achieved in the understanding of the phenomena which occur in ferromagnets in the case of parallel excitation of spin waves. Physical ideas developed in this connection are also valid for a number of other similar problems.

This refers above all to nonlinear phenomena in the case of "transverse" excitation of spin waves, i.e., the parametric excitation of spin waves by homogeneous precession of magnetization. In the simplest case of first order instability and ferromagnetic resonance ($\omega_0 \approx \omega_p \approx 2\omega_k$) the main nonlinear mechanism is the reaction of spin waves on homogeneous precession^[22].

Well away from the resonance, the phenomena which occur during transverse excitation are essentially similar to those found for parallel excitation. It is shown in^[22] that the interaction of the waves with one another is appreciable even at small excesses above the threshold. All three nonlinear damping mechanisms discussed in Sec. 3 play an important role in this connection. A substantial volume of experimental data is now available in this field, but detailed comparisons with the theory are inhibited by various complicating factors.

In particular, even in the linear approximation, the dependence of γ on θ and $|k|$ means that the question as to which waves are excited first is difficult to answer.

For second-order instability, $\omega_0 \approx \omega_p = \omega_k$, two-magnon scattering plays an important role in addition to the above factors and must be taken into account at the same time as the pair interaction. For large excesses above the threshold, this is accompanied by phenomena which are not as yet understood, for example, the "valley" on the resonance curve^[68].

The phenomena observed in the course of parametric excitation of spin waves in antiferromagnets are at least in principle, much richer because of the presence of several spectrum branches.

Cubic antiferromagnets with weak anisotropy, and uniaxial antiferromagnets of the "easy plane" type, are of particular interest and have been investigated by

Seavey^[69], Borovik-Romanov and Prozorova^[70], and Ozhogin^[71]. It is shown in^[72, 73] that all the predictions of the S theory are fully applicable to antiferromagnets. The interpretation of experimental results is complicated by the fact that defects play an important role in typical experimental situations involving antiferromagnets.

An interesting and important range of problems is associated with the study of the parametric excitation of waves in media with large scale (in comparison with the wavelength) inhomogeneities. In this case, we have an additional "linear" limiting mechanism because of the loss of energy to the region with the higher threshold. This mechanism was investigated in detail in^[74] in the case of waves in plasmas. It is also important to note the interesting phenomenon of parametric echo which is observed during transverse excitation in weakly inhomogeneous ferromagnets. A qualitative explanation of this phenomenon is given in^[75]. It would be interesting to elucidate the role of wave interaction using short intense pump pulses. Studies in this area may be of practical importance in the sense that they may lead to the development of amplifiers, amplifying delay lines, and other devices for pulse shaping.

The importance of the theory outlined in the present review extends beyond the framework of ferromagnetism. It is, essentially, the general theory of parametric excitation of waves in nonlinear media with a nondecay spectrum. In particular, it is valid for certain problems in the physics of plasmas,^[76] and can be used to investigate the parametric excitation of waves on the surface of a liquid. It is therefore hoped that this theory reflects many of the essential features of turbulence established in an unstable continuous medium when the excess above the threshold is not too large.

¹⁾We note that the dependence of χ' and χ'' on h^2 found in^[46] is qualitatively in agreement with Fig. 5 for all excesses above the threshold with the exception of the ~ 1.2 dB region near the threshold.

²⁾We note that the definition of S_0 given by (4.3) is the same as the definition $S_{1/2\pi}, \chi_{1/2\pi} \equiv S_{11}$ (Eq. (3.20)).

³B. B. Kadomtsev and V. I. Karpman, Usp. Fiz. Nauk 103, 193 (1970) [Sov. Phys.-Usp. 14, 40 (1971)].

⁴Rayleigh, Theory of Sound (Russ. Transl., Gostekhizdat, M., 1955, Vols. I-II), Dover, N.Y.

⁵N. Bloembergen and R. Damon, Phys. Rev. 85, 699 (1952); N. Bloembergen and S. Wang, Phys. Rev. 93, 72 (1954).

⁶H. Sühl, J. Phys. Chem. Solids 1, 209 (1957).

⁷F. R. Morgenthaler, J. Appl. Phys. 31, 95S (1960).

⁸E. Schrödmann, J. Green, and U. Milano, J. Appl. Phys. 31, 386S (1960).

⁹V. N. Oraevskii and R. Z. Sagdeev, Zh. Tekh. Fiz. 32, 1291 (1962) [Sov. Phys.-Tehn. Phys. 7, 955 (1963)].

¹⁰N. Bloembergen, Nonlinear Optics (Russ. Transl., Mir, M., 1966).

¹¹V. P. Silin, Usp. Fiz. Nauk 104, 677 (1971) [Sov. Phys.-Usp. 14, 538 (1972)].

¹²I. E. Andreev, A. N. Kiril', and V. P. Silin, Zh. Eksp. Teor. Fiz. 57, 1024 (1969) [Sov. Phys.-JETP 30, 559 (1970)].

¹³V. E. Zakharov, Zh. Eksp. Teor. Fiz. 51, 1107 (1966) [Sov. Phys.-JETP 24, 740 (1967)].

¹⁴V. E. Zakharov, Zh. Prikl. Mekh. Tekh. Fiz. No. 2, 80 (1968).

- ¹³T. V. Bengamen and I. E. Feir, *J. Fluid Mech.* **27**, 417 (1967).
- ¹⁴D. Witham, in: *Nonlinear Theory of Plasma Propagation* (Russ. Transl., Mir, M., 1970).
- ¹⁵F. Bertaut and F. Forrat, *C. R. Acad. Sci. (Paris)* **242**, 382 (1956).
- ¹⁶S. Geller and M. A. Gillo, *Acta Crystallogr.* **10**, 239 (1957).
- ¹⁷E. Schlömann, *Phys. Rev.* **116**, 829 (1959).
- ¹⁸J. D. Bierlein and P. Richards, *Phys. Rev. B*, **1**, 4342 (1970).
- ¹⁹V. E. Zakharov, V. S. L'vov, and S. S. Starobinets, *Fiz. Tverd. Tela* **11**, 2047 (1969) [Sov. Phys.-Solid State] **11**, 1658 (1970)].
- ²⁰V. E. Zakharov, V. S. L'vov, and S. S. Starobinets, *Zh. Eksp. Teor. Fiz.* **59**, 1200 (1970) [Sov. Phys.-JETP] **32**, 656 (1970)].
- ²¹V. E. Zautkin, V. S. L'vov, S. L. Musher, and S. S. Starobinets, *ZhETF Pis'ma Red.* **14**, 310 (1970) [JETP Lett.] **14**, 206 (1970)].
- ²²V. S. L'vov and S. S. Starobinets, *Fiz. Tverd. Tela* **13**, 523 (1971) [Sov. Phys.-Solid State] **13**, 418 (1971)].
- ²³V. E. Zautkin, V. E. Zakharov, V. S. L'vov, S. L. Musher, and S. S. Starobinets, *Zh. Eksp. Teor. Fiz.* **62**, 1782 (1972) [Sov. Phys.-JETP] **35**, 926 (1972)].
- ²⁴V. E. Zakharov, V. S. L'vov, and S. L. Musher, *Fiz. Tverd. Tela* **14**, 832 (1972) [Sov. Phys.-Solid State] **14**, 710 (1972)].
- ²⁵T. S. Hartwick, E. R. Peressini, and M. T. Weiss, *J. Appl. Phys.* **32**, 223 (1960).
- ²⁶V. S. L'vov, S. L. Musher, and S. S. Starobinets, *Zh. Eksp. Teor. Fiz.* **64**, 1074 (1973) [Sov. Phys.-JETP] **37**, 546 (1973)].
- ²⁷V. V. Zautkin, V. S. L'vov, and S. S. Starobinets, *Zh. Eksp. Teor. Fiz.* **63**, 182 (1972) [Sov. Phys.-JETP] **36**, 96 (1973)].
- ²⁸H. Le Gall, B. Lemire, and D. Sere, *Solid State Commun.* **919** (1967).
- ²⁹V. V. Kveder, B. Ya. Kotyuzhanski, and L. A. Prozorova, *Zh. Eksp. Teor. Fiz.* **63**, 2205 (1972) [Sov. Phys.-JETP] **36**, 1165 (1973)].
- ³⁰T. Holstein and H. Primakoff, *Phys. Rev.* **58**, 1098 (1940).
- ³¹A. Akhiezer, V. Bar'yakhtar, and S. Peletinskii, *Spinovye volny (Spin Waves)*, Nauka, M., 1967.
- ³²V. E. Zakharov, V. S. L'vov, and S. S. Starobinets, *Fiz. Tverd. Tela* **11**, 2922 (1969) [Sov. Phys.-Solid State] **11**, 2368 (1970)].
- ³³V. S. L'vov, Preprint No. 7-73, Institute of Nuclear Physics, Siberian Branch, USSR Academy of Sciences, Novosibirsk. 1973.
- ³⁴V. E. Zakharov and V. S. L'vov, *Fiz. Tverd. Tela* **14**, 2913 (1972). [Sov. Phys. Solid State] **14**, 2513 (1973)].
- ³⁵E. Schloman, *J. Appl. Phys.* **33**, 527 (1962).
- ³⁶P. Gottlieb and H. Sühl, *J. Appl. Phys.* **33**, 1508 (1962).
- ³⁷Ya. A. Monosov, *Nelineinyy ferromagnitny rezonans (Nonlinear Ferromagnetic Resonance)*, Nauka, M., 1971.
- ³⁸G. A. Melkov, *Zh. Eksp. Teor. Fiz.* **61**, 373 (1971) [Sov. Phys.-JETP] **34**, 198 (1972)].
- ³⁹T. Kohane and E. Schlömann, *J. Appl. Phys.* **34**, 1554 (1963).
- ⁴⁰A. V. Vashkovskii and Ya. A. Monosov, *Radiotekhnika i Elektron.* **12**, 1392 (1967); I. A. Deryugin, N. I. Lyashenko, and L. L. Stakhurskii, *Radiotekhnika i Elektron.* **14**, 1514 (1969).
- ⁴¹H. Le Gall, J. P. Jamet, and V. Cagan, *Solid State Commun.* **7**, 27 (1969); *J. Appl. Phys.* **40**, 1505 (1969).
- ⁴²V. N. Agartanov, V. B. Antipov, V. V. Kolpakov, and E. M. Fedorin, *Fiz. Tverd. Tela* **14**, 2446 (1972) [Sov. Phys.-Solid State] **14**, 2116 (1973)]; V. N. Agartanov and E. M. Fedorin, *Fiz. Tverd. Tela* **15**, 579 (1973) [Sov. Phys.-Solid State] **15**, 402 (1973)].
- ⁴³A. G. Gurevich, G. M. Drabkin, I. M. Lazebnik, E. I. Mal'tsev, I. I. Marchik, and S. S. Starobinets, *Fiz. Tverd. Tela* **10**, 647 (1968) [Sov. Phys.-Solid State] **10**, 511 (1968)].
- ⁴⁴L. D. Landau, *Sb. trudov (Collected Works)* Vol. I, Nauka, M., 1969, p. 447.
- ⁴⁵G. A. Petrakovskii and V. N. Berzhanskii, *ZhETF Pis'ma Red.* **12**, 429 (1970) [JETP Lett.] **12**, 298 (1970)].
- ⁴⁶Ya. A. Monosov and V. V. Surin, *Zh. Eksp. Teor. Fiz.* **65**, 1905 (1973) [Sov. Phys.-JETP] **38**, 951 (1974)].
- ⁴⁷J. J. Green and B. J. Healy, *J. Appl. Phys.* **34**, 1285 (1963).
- ⁴⁸V. S. L'vov, Preprint No. 69-72, Institute of Nuclear Physics, Siberian Branch, USSR Academy of Sciences, Novosibirsk, 1972.
- ⁴⁹V. S. L'vov, Preprint No. 73, Institute of Nuclear Physics, Siberian Branch, USSR Academy of Sciences, Novosibirsk, 1973.
- ⁵⁰W. E. Courtney and P. I. Claricoats, *J. Electron. Control* **16**(1), 1 (1964).
- ⁵¹V. V. Surin, Candidate's Dissertation, IRE AN SSSR, 1969.
- ⁵²A. P. Safant'evskii, Candidate's Dissertation, IRE AN SSSR, 1971.
- ⁵³S. Wang, G. Thomas, and Ta-lin Hsu, *J. Appl. Phys.* **39**, 2719 (1968); S. Wang and Ta-lin Hsu, *Appl. Phys. Lett.* **16**, 534 (1970).
- ⁵⁴J. J. Green and E. Schlömann, *J. Appl. Phys.* **33**, 1358 (1962).
- ⁵⁵V. V. Zautkin and S. S. Starobinets, *Fiz. Tverd. Tela* **16** (1974) [Sov. Phys.-Solid State] **16**, (1974)].
- ⁵⁶V. E. Shapiro, I. P. Shaptev, and R. G. Khlebopros, Preprint No. 19, Institute of Physics, Siberian Branch, USSR Academy of Sciences, Krasnoyarsk, 1970.
- ⁵⁷M. Sparks, *Ferromagnetic Relaxation Theory*, N.Y., 1964.
- ⁵⁸E. Schlömann, *Phys. Rev.* **182**, 632 (1969).
- ⁵⁹H. Suhl, *J. Appl. Phys.* **30**, 1961 (1959).
- ⁶⁰E. Schlömann, *Phys. Rev.* **116**, 828 (1959).
- ⁶¹A. Palacino, J. Waugh, and J. Green, *J. Appl. Phys.* **37**, 3337 (1966); Q. H. F. Vrechen, *J. Appl. Phys.* **40**, 1849 (1969); G. E. Patton, *J. Appl. Phys.* **41**, 1637 (1970); D. E. Scotter, *J. Appl. Phys.* **42**, 4088 (1971).
- ⁶²V. E. Zakharov and V. S. L'vov, *Zh. Eksp. Teor. Fiz.* **60**, 2066 (1971) [Sov. Phys.-JETP] **33**, 1113 (1971)].
- ⁶³V. S. L'vov, *Fiz. Tverd. Tela* **13**, 3488 (1970) [Sov. Phys.-Solid State] **13**, 2949 (1972)].
- ⁶⁴V. S. L'vov and A. M. Rubenchik, Preprint No. 1-72, Institute of Nuclear Physics, Siberian Branch, USSR Academy of Sciences, Novosibirsk, 1972.
- ⁶⁵V. S. L'vov, A. M. Rubenchik, V. V. Sobolev, and V. S. Synakh, *Fiz. Tverd. Tela* **15**, 793 (1973) [Sov. Phys.-Solid State] **15**, 550 (1973)].
- ⁶⁶V. E. Zakharov, V. V. Sobolev, and V. S. Synakh, *ZhETF Pis'ma Red.* **14**, 564 (1971) [JETP Lett.] **14**, 390 (1971)].
- ⁶⁷V. N. Vlasov, V. A. Petrishchev, and V. I. Talanov, *Izv. Vyssh. Uchebn. Zaved. Radiofiz.* **14**, 1353 (1971).
- ⁶⁸A. G. Gurevich and S. S. Starobinets, *ZhETF Pis'ma Red.* **39**, 1075 (1968) [sic!].
- ⁶⁹M. H. Seavey, *Phys. Rev. Lett.* **23**, 132 (1969).
- ⁷⁰L. A. Prozorova and A. S. Borovik-Romanov, *ZhETF*

- Pis. Red. 10, 316 (1969) [JETP Lett. 10, 201 (1969)].
⁷¹V. I. Ozhogin, Zh. Eksp. Teor. Fiz. 48, 1307 (1965)
[Sov. Phys.-JETP 21, 874 (1965)]; 58, 2079 (1970)
[Sov. Phys.-JETP 31, 1121 (1970)].
⁷²V. A. Kolanov, V. S. L'vov, and M. I. Shirokov, ZhETF
Pis. Red. 19, 680 (1974) [JETP Lett. 19, 351 (1974)].
⁷³V. S. L'vov and M. I. Shirokov, Preprint No. 14, IAiE
SO AN SSSR, Novosibirsk, 1974.

- ⁷⁴M. N. Rosenbluth, Phys. Rev. Lett. 29, 565 (1972).
⁷⁵G. E. Herrman, R. M. Hill, and D. E. Kaplan, Phys.
Rev. B, 2, 2587 (1970).
⁷⁶V. S. L'vov and A. M. Rubenchik, Zh. Eksp. Teor. Fiz.
64, 515 (1973) [Sov. Phys.-JETP 37, 263 (1973)].

Translated by S. Chomet.